ABSTRACT

HUNT, MICHAEL CODY. Millponds: An Archive for Post-Colonial Storm Histories. (Under the direction of Dr. Elana Leithold).

Extreme storm events and their widespread socioeconomic effects have been well documented in recent U.S. history, but prior to 1870 few records are available. Previous reconstructions have been attempted based on lake and tree-ring records, but these are only possible in a limited number of locations, minimizing their utility for forecasting models and regional planning. In the Eastern U.S, however, millponds were extremely widespread from the colonial period until the early 1900's. In this study the potential use of event layers within millpond sediments as storm proxies has been investigated. Grain size analyses were used to identify coarser (sand/silt) event layers, as opposed to the "background" pond sediment, which is relatively fine-grained (fine silt and clay). These changes in the grain-size distribution of millpond sediments are interpreted to indicate fluctuations of inlet and outlet stream discharge, primarily as a result of large precipitation events. Millpond sediments were examined along stream banks and in piston cores from five sites in Wake County, North Carolina, and the presence and thickness of coarser event layers were documented based on field observations and laser particle size analyses. The age of the sediments was determined by a combination of tree ring chronology, historical records, and ^{210}Pb analysis. GIS was used to determine coring locations and to detail the morphological characteristics of the millponds in order to help with interpreting the profiles/cores. This study has identified graded storm layers at multiple millpond sites that indicate extreme hydrologic events. Some of these layers correlate with storms in the historical record, but many do not. The

identification of storm layers in millpond sediments may lead to reconstruction of storm histories in many other areas.

Millponds: An Archive for Post-Colonial Storm Histories

by
Michael Cody Hunt

A thesis submitted to the Graduate Faculty of
North Carolina State University
in partial fulfillment of the
requirements for the degree of
Master of Science

Marine, Earth, and Atmospheric Sciences

Raleigh, North Carolina

2011

APPROVED BY:

_______________________________ _______________________________
Karl Wegmann Chris Osburn

____
Elana L. Leithold
Committee Chair

DEDICATION

This thesis is dedicated to my wife and daughter, who have offered me unconditional love and support throughout the course of this thesis. It is also dedicated to my father and mother, who taught me the value of hard work and perseverance.

BIOGRAPHY

I was born on July 22, 1985 to Michael Coward Hunt and Felicia Ann Hunt in Lumberton, NC. My Native American heritage played an integral role in my career path early on. During my youth, I spent a large portion of my leisure time in the woods and on the waterways just as my Lumbee ancestors before me. Through my cultural heritage and love of the outdoors, I gained a respect and affection for nature which fostered my desire to pursue a career in the earth sciences.

My collegiate career began in 2003 at the University of North Carolina at Pembroke, and eventually after various stints of full-time work, I graduated with a B.S. in Geology from the University of North Carolina at Charlotte. After my graduation, I enrolled in the Marine, Earth, and Atmospheric Sciences program at North Carolina State University. I am very grateful to have had the opportunity to attend these excellent North Carolina universities and the experiences gained have helped to prepare me for the challenges I will face in my career and life.

ACKNOWLEDGMENTS

I would first like to acknowledge and show my gratitude to those who helped guide me through this process, my committee members. Dr. Karl Wegmann thank you for helping me identify this project and for the usage of your equipment and lab materials. Dr. Chris Osburn, I appreciate the guidance and critique you have given me throughout this process. I would like to especially thank my advisor Dr. Elana Leithold for her support and commitment to my project and graduate career throughout the past couple of years.

To my lab partner Katherine Ryker, I appreciate the time and effort you gave in helping me to understand the lab techniques and instruments some of which were integral to my thesis project. The eagerness with which you have to help others, especially me, is something I admire and will as remember. To John Michaels and Robert Lewis I appreciate the time and help you dedicated to me and my project, especially help with the dirty, hot field tasks I burdened you with. Also, to Dr. Demaster, I appreciate your help and guidance in using your lab for the ^{210}Pb dating methods used in this project.

Most of all, I'd like to thank my wife and daughter whom have weathered the storm that is a thesis project with me, and given me the kind of love and support that I needed through these last couple of years. To Andrea, thank you especially for respecting the time and devotion it has taken for us to get here and for the support you have given me. Lastly, I would like to thank all of my colleagues, professors, and students whom have made my experience at North Carolina State University unforgettable and enjoyable.

TABLE OF CONTENTS

LIST OF TABLES

LIST OF FIGURES

1.0 INTRODUCTION

The region of eastern North America between the Appalachian Mountains and Atlantic Coastal Plain is known as the Piedmont and includes high population areas such as Atlanta, Georgia, Greenville, South Carolina, and the Research Triangle and Triad metropolitan centers of North Carolina. Throughout the Southeastern Piedmont the occurrence of storms has been recorded since European settlement, and these records form the basis of forecasting models, climate predictions, and disaster planning. The earlier parts of the record, from about 1586 to 1870, however, have proven to be inaccurate and geographically biased towards areas of higher population concentrations (typically coastal areas) (Hudgins 2000; Storen et al., 2010).

Severe storm events account for millions of dollars in damages to North Carolina annually (State Climate Office of North Carolina, 2010). To plan/prepare for these storms, residents rely on long-term and short-term (or single event) forecasting models whose accuracy is directly related to the historical data they utilize. Prior to about 1870, actual measurements (i.e. precipitation amounts, pressure, wind speed, etc.) were not made and up to 1910 most of the available information is from newspaper accounts (Hudgins, 2000) from which the coverage and presentation of detail varied greatly from one storm event to another. Furthermore, most of the observations were made along the North Carolina coastal plain, and the recorded storms may not have coincided with those that had the greatest effects in the Piedmont region.

Previous research in other regions has shown that lacustrine sediments may contain valuable proxy records of high-intensity storm events (Campbell, 1998; Brown et al., 2000; Noren et al., 2000; Osleger et al., 2009; Czymzik et al., 2010). There are no naturally occurring lakes in the Piedmont of North Carolina, but during the period just before the American Revolution (1776) to the onset of the Industrial Revolution (mid-late 19th century), hundreds of mills were in operation across the state (US Census Bureau, 1870). The hypothesis of this thesis is that the ponds associated with historic mills could preserve sedimentary records of extreme precipitation events. To test this hypothesis, the sedimentary fills of multiple millponds were sampled in an attempt to reconstruct the post-colonial storm history of Wake County, North Carolina. To identify potential sites, industrial maps of the mills in Wake County were used including two that were made during the height of mill proliferation, the first by Fendol Bevers in 1871 and the second by A. W. Shaffer in 1887. The sites investigated included five millpond sites within the Neuse River Basin, Wake County, NC: 1) Cook's, 2) Betty's (unofficial name), 3) JD Hayes', 4) Yates', and 5) Mitchell Mills (Figure 1.1).

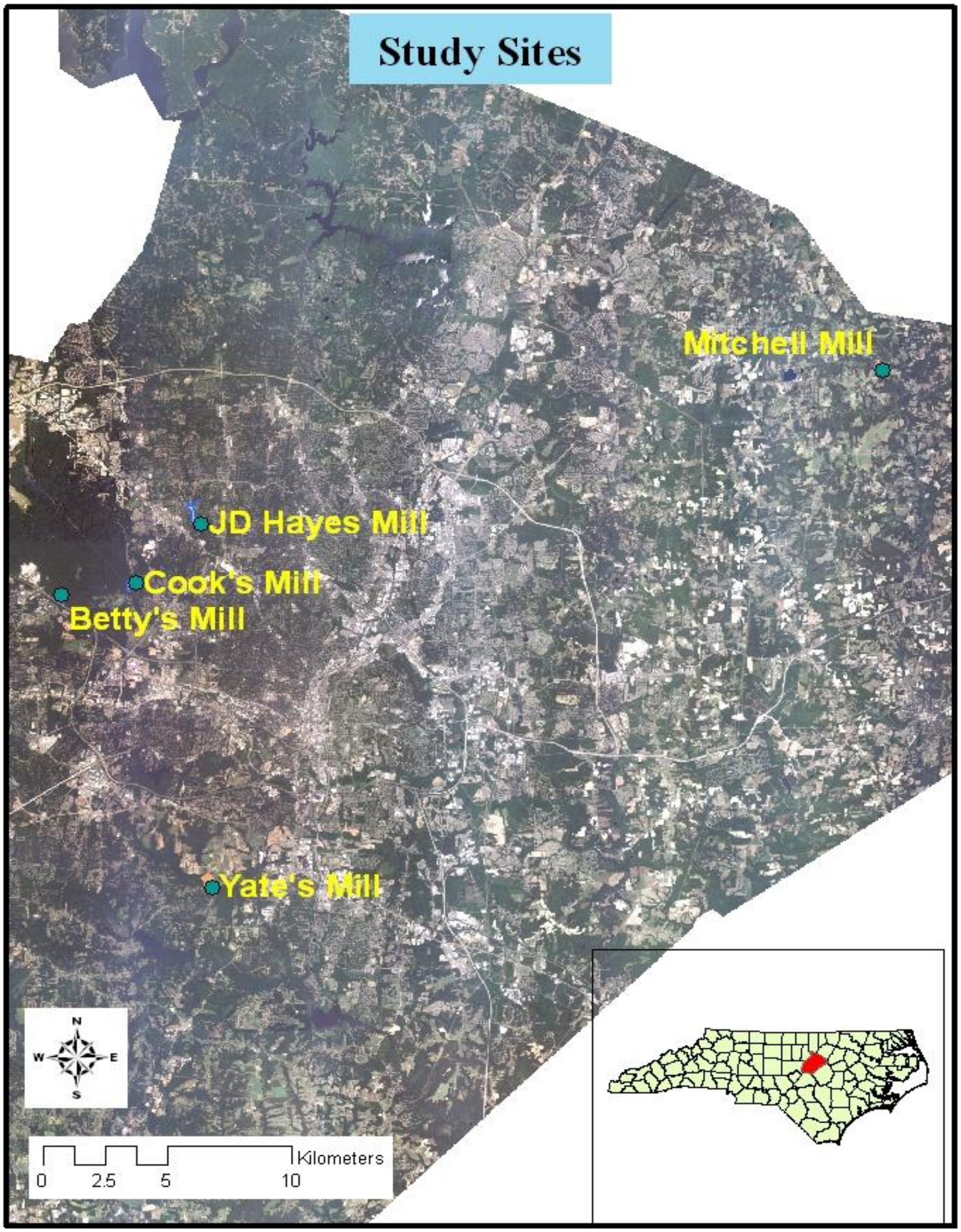

Figure 1.1 Millpond study site locations in Wake County, NC. From North to South: Mitchell, JD Hayes, Cook's, Betty's, and Yates' Mills.

2.0 BACKGROUND

2.1 Millpond Stratigraphy

Dam building for water-powered mills began in the eastern US in the late 1600s and persisted until the early 20th century, resulting in >65,000 mills by 1840 (Walter et al., 2007). In North Carolina's agriculturally based society, mills were a necessity to grind corn and wheat, and they proliferated with hundreds in operation at their peak abundance (O'Driscoll et al., 2006; North Carolina State Archives).

These ponds effectively created a series of slack water reservoirs which trapped and stored sediment as it eroded from the surrounding landscape (Schenk and Hupp, 2009). Millpond deposits typically rest on wetland sediments and range from 1-5 meters thick. They are composed of silt and clays, with thin, interstratified sand layers (Walter and Merritts, 2008; Michelsen 2009). Similar deposits have been described throughout the Piedmont from Pennsylvania to South Carolina, and within the study area in Wake County, NC (Kautzman, 1972). As summarized by Walter and Merritts (2008): "The bedrock (weathered) valley floor typically is overlain by: (i) a thin (<0.5-m) bed of angular to subangular quartz-rich gravel; (ii) a thin (<0.5- to 1-m), dark (black, 10YR 2/1, Munsell soil classification), organic-rich silt loam; and (iii) a thick (1- to 5-m) pale to yellowish brown sequence of fine sand, silt, and clay commonly referred to as silt loam and clay loam."

With time, many of the milldams have been removed or have breached through neglect. The initial result is that the stream channel rapidly incises to pre-colonial levels (usually bedrock) and exposes several meters of millpond deposits. Another long-term result is that sedimentation behind the milldam has elevated the original floodplain level above the channel, thus diminishing the sediment sink function of the floodplain (Schenk and Hupp, 2009). Evidence for isolation of the floodplain from the channel includes the occurrence of root crowns at the soil surface which indicates a static floodplain elevation (Jackson et al., 2005). Since the top surface of the millpond deposits has remained relatively unchanged, one can assume that this level correlates with the level to which sediment had built up before dam breaching. Similarly, the base of the fine-grained millpond sediments is reasonably assumed to have been deposited soon after the construction date of the milldam at a particular site.

2.2 Lacustrine "Event" Layers

Fine-grained lake deposits are commonly punctuated by thin sand (or silt) layers. These layers are typically coarser, contain more macrofossils of terrestrial plants than the 'background' fine-grained sediments, and are commonly normally graded (Brown et al., 2000; Noren et al., 2002; Osleger et al., 2009). The layers are interpreted to record storm events (flooding, high intensity rains, etc.).

Clastic sediment carried by inlet streams is typically dispersed from the shoreline to deeper parts of lakes by surface or subsurface plumes of suspended sediment, or less typically by sloughing of the lake margins (Brown et al., 2000; Campbell, 1998). During "normal" flow conditions any sand or coarser particles in motion within the streams typically accumulate proximal to the stream mouths, and only fine-grained clays and silts are deposited on the deeper lake floor. During exceptional runoff events, however, sand-sized material may be deposited further lakeward (Hart and Long, 1990; Seilacher and Aigner, 1991; Noren et al., 2002; Nichols, 2009). Czymzik et al. (2010), for example, showed that spring floods, associated with torrential downpours in Lake Ammersee, Germany were recorded by coarse grained, normally graded sediment layers. At Lake Tahoe (U.S.), Osleger et al. (2008) identified coarse-grained turbidites interstratified with fine-grained 'background' sediments. They interpreted these "turbidites" as the result of the rapid influx of sediments delivered to the lake by high-intensity storms.

As stream velocity increases with increasing discharge, larger sediment grains are transported in the stream's suspended load, and when the sediment load is carried into the still water of a lake, the coarser suspended sediment will settle out and be deposited on the lake bed (Campbell, 1998; Nichols, 2009). It has been shown by Campbell (1998) that, if a lake is small enough to have a relatively short mean lake water residence time and the outlet stream flows quickly enough, fine clays are removed from the lake before they are deposited. Thus in small lakes, changes in the clastic grain-size distribution of the sediments on the lake floor may indicate fluctuations of inlet and outlet stream discharge. Even sediment redistributed from the shoreline into deeper water by processes such as sloughing will be subject to such sorting, with the coarsest sediment that is transported to mid-lake being determined by the strength of fluid flows (Kautzman, 1972; Campbell, 1998).

Density currents may also transport coarse sediments across lake floors (Nichols, 2009). When the density of the sediment-water mixture of the input stream is denser than the lake waters and there is a sufficient slope at the stream mouth, sediment-gravity flows may form (Sturm and Matter, 1978; Czymzik et al., 2010). As the turbidity current spreads across the lake floor, the density difference diminishes, leading to a reduced transport capacity, and consequently, successively finer grain sizes are deposited (Siegenthaler and Sturm, 1991; Nichols, 2009; Czymzik et al., 2010).

In summary, whether sediments are transported into lakes by surface plumes or by sediment-gravity flows, grain size trends may be used to identify past high stream-discharge events. The grain-size record of lake sediments may therefore be a proxy of changes in storminess over time, a record that may be particularly clear near the inlet of a stream (Campbell, 1998; Nichols, 2009).

2.3 Study Area and the Neuse River Basin

The Neuse River begins in Person and Orange Counties in the Piedmont region of North Carolina and flows about 400 km to the Pamlico Sound (Phillips, 1992). The Neuse is the third largest river basin in North Carolina, containing approximately one-sixth of the state's population, and has an area of 16,150 km^2, draining 5,628 km of streams (NCWRC, 2011). Approximately 45% of the basin is forested, 13% is considered urban and 29% crop and pasture land (NCDWQ, 2001).

Although the topography of the Piedmont region is not as rugged as that of the Blue Ridge, surface and stream gradients are sufficient to produce flood flow velocities of 1.5 to 3 m/s. The combination of intense rains coupled with the province's steep gradients and highly erodible soils produces some of the highest concentrations of fluvial sediment (bedload and suspended) measured in North Carolina streams (Simmons, 1988), with basin wide sediment yields ranging from 275-330 Tons km^{-2} yr^{-1} (Phillips, 1992). Depending on storm intensity and the size of a drainage basin, Piedmont streams might remain at flood stage from a few hours to several days (Simmons, 1988).

In the study area, the soil profile lies above saprolite weathered from the underlying bedrock and are often 1.5 m or more in thickness (Phillips, 1992). The fine-grained clayey soils of the Piedmont are typically composed of predominately kaolinite and/or smectite clay (Daniels, 1999). Sand in Piedmont alluvium is dominated by quartz, but includes significant amounts of feldspar (Benedetti et al., 2006).

The bedrock of the study area is a complex interlayered sequence of high and low-grade metamorphic rocks oriented in a northeast trending belt known locally as the Raleigh Belt. Included in this sequence are phyllites, metatuffs, volcanic flow rocks, mafic and felsic gneisses, and schists, which originally were a volcanic-sedimentary succession composed of lithologies with a wide range of composition and areal distribution. In the northern part of Wake County, there are a series of deformed ultramafic rocks caused by the intrusion of felsic plutons (Wilson, 1981).

3.0 HISTORY OF THE MILLPOND SITES

Cook's Mill Dam is located on Richland Creek in Umstead State Park, NC. The pond no longer exists but at one time extended upstream from the base of a dam that is located directly beneath the Ebenezer Church Road bridge (Figure 5.1). Deed records indicate that the mill was most likely originally petitioned by James Kimbrough in 1798 (North Carolina State Archives). The mill dam was breached in or very near 1910 according to landowner accounts and tree chronologies. The relic mill pond sediments are now exposed along the bank of Richland Creek (Figure 5.1).

Located on Reedy Creek in Umstead State Park, NC, Betty's Mill (Figure 5.2) is not recorded on the Fendol Bevers map of 1871. Since it is not shown on the map and does not appear in historical records, the site was named for the Umstead Park ranger who originally discovered its location (personal comm., Karl Wegmann, 2010). Since the dam was constructed of dry-stacked stone without mortar, it is inferred to have been constructed prior to about 1810 (personal comm., Doug Swords, 2010). A profile through the former millpond sediments is exposed along the bank of Reedy Creek (Figure 5.2).

Yates' Mill (Figure 5.3) is an active mill site, and is currently the location of a park maintained by the Wake County Parks Division. The park is located on Steep Hill Creek at the intersection of Yate's Mill Pond Road and Lake Wheeler Road in Raleigh, NC. Samuel Peterson founded the mill around 1756 ca. (or shortly before) according to land records and the dam remained in working condition until September, 6, 1996 when it was breached during Hurricane Fran. The county restored the mill and its grinding machinery in 2005 (Wake County, 2011). During the restoration efforts, the inner portion of the pond was dredged while a buffer of several meters near the margins was left untouched for riparian habitat (personal comm., Rebeccah Cope, 2010).

JD Hayes is a relic pond site located on Hairy Snipe Creek downstream from Wooten Meadows Playground in Raleigh, NC (Figure 5.4). This property was originally deeded as a mill to Moses Parks, but was built by three merchant millers/investors, Richard Heartsville, Nathaniel Kimbrouch, and John Hartsvield in 1773 (North Carolina State Archives). The mill appears on the Fendol Bevers map of 1871 but is absent from the 1887 Shaffer's map, furthermore the 1870 Industrial Census lists a J Hays mill with a 4x20 foot overshot wheel (US Census Bureau, 1870). The milldam must have breached between 1871 and1887, and after its breach, the site was relatively undisturbed, as it had been a farmland for most of the time and now a park (personal comm., Victor Lebsock, 2010).

Now the site of a state park located on the Little River, Mitchell Millpond, located off Mitchell Mill Rd. in Rolesville, NC, (Figure 5.5) has also remained relatively undisturbed, as the surrounding land usage has always been agricultural. Petition records state that Josiah Crudup requested that a "mill be built at a large flat rock," now known to be an exposure of the Rolesville batholith, around 1772 (North Carolina State Archives). However, the owner of the mill has stated that according to his family's records, the mill was built without a petition in 1759 (personal comm., Doug Swords, 2010).

4.0 METHODS

4.1 ArcGIS Mapping

A geographic information system (GIS) was used to digitize the areal extent of the millponds, calculate stream slopes, and to determine which recorded storms passed near the study sites. The software package used was Arc GIS 9.3, published by ESRI. At Yates and Mitchell millponds, where ponds still exist, the extent of the original millpond was mapped for comparison. A digital elevation model (DEM) of Wake County, NC with 3 m resolution (cell size) was obtained from the United States Department of Agriculture's (USDA) Natural Resources Conservation Service (NRCS): Geospatial Data Gateway. Digitization of the relic millponds was performed by creating a two- meter- interval topographic map using the DEM. The dam height and ortho imagery was then used to digitize an estimation of the extent of the relic millponds. Ortho imagery and a polygon file of the soils of Wake County were also obtained from NRCS. Shapefiles of the water-bodies, roads, and geology of Wake County were obtained from the Wake County Government. All sample sites and milldam locations were added as XY data to the map, from coordinates logged in the field using a handheld Magellan Triton global positioning system (GPS). A shapefile of storm tracks (hurricanes and tropical systems) through North Carolina since 1851 was provided by the State Climate Office.

4.2 Sample Collection

Mill-pond deposits (Figure 4.1) were examined and sediment samples were collected in one of two ways:

1) Coarser event layers and background sediments were manually sampled at stream-bank outcrops at the Cook's and Betty's mill locations (Figure 4.1) using a small spatula. At each site the profile was logged in a field book, with the exact stratigraphic position of each coarse layer noted. The samples were placed in small plastic bags, labeled, and stored in a freezer.

2) A hammer driven piston-corer (Figure 4.1), called a Geo-Corer (Volnout, 2011) was used at the Yates Mill, J.D. Hayes Mill, and Mitchell Mill sites where stream-bank outcrops were not available. The coring device employs 1 meter long and 3.8 cm diameter aluminum core barrels, which if used in succession are capable of retrieving cores to a depth of 25 meters from the surface of a 10 meter deep lake (http://www.geo-corer.com/basicsystem.htm). The auger bit used is unable to core through coarse sediments (e.g., coarse sand or gravel), so the sample tubes were driven to a depth of refusal at all locations which corresponds to sandy channel deposits and/or bedrock. All core tubes were brought to the lab and stored in a walk-in refrigerator unit until further analysis. In the lab, cores were extruded, sampled at 1 cm intervals, placed in plastic bags, and stored in a freezer.

Bank Measurements

Geo-Coring

Figure 4.1 Left: Cook’s Millpond sediments being sampled at a bank outcrop; Right: Geo-corer set up for coring at Yates’ Millpond.

4.3 Sample Preparation and Grain Size Analysis

Bulk samples from each of the intervals sampled at the Betty's and Cook's Mill outcrops and from every-other interval in the Yates Mill, J.D. Hayes Mill, and Mitchell Mill cores were frozen before being prepared for particle size analysis. The samples were thawed at room temperature and approximately 1-2 g of sediment was sieved through a clean 2 mm stainless steel sieve with 40-50 ml of deionized (DI) water into a clean 50 ml beaker, to remove any large organic material (OM). The samples were dried in a low temperature oven (~ 50°C) for a period of 1-2 days. In order to remove any remaining OM, samples were treated with 20-25 ml of 30% hydrogen peroxide for a period of 4-7 days or until oxidation ceased (see Figure 4.2).

Grain size analysis was conducted on the organic free samples using a Beckman Coulter LS 13-320 laser particle size analyzer (LPSA). The instrument uses a laser light source to illuminate particulates within a sample cell and the light scattered by the particles is then detected by silicon photo-detectors. The intensity of light at each detector is measured as a function of angle and then is subjected to mathematical analysis where the end result is a particle size distribution. The dried sediment samples were suspended in water and disposable polyethylene pipettes were used to transfer an appropriate sample volume, usually 1-4 ml of solution, to the Universal Liquid Module of the LPSA until 40-50% obscuration of the beam was reached. Once the appropriate obscuration was achieved, the water column was sonicated for 15 seconds and analyzed for 60 seconds. The Beckman Coulter software calculated the percent volume within pre-set size intervals, from 0.03999 to 2000 μm. The software also calculates relative statistics for each sample including mean and median grain size.

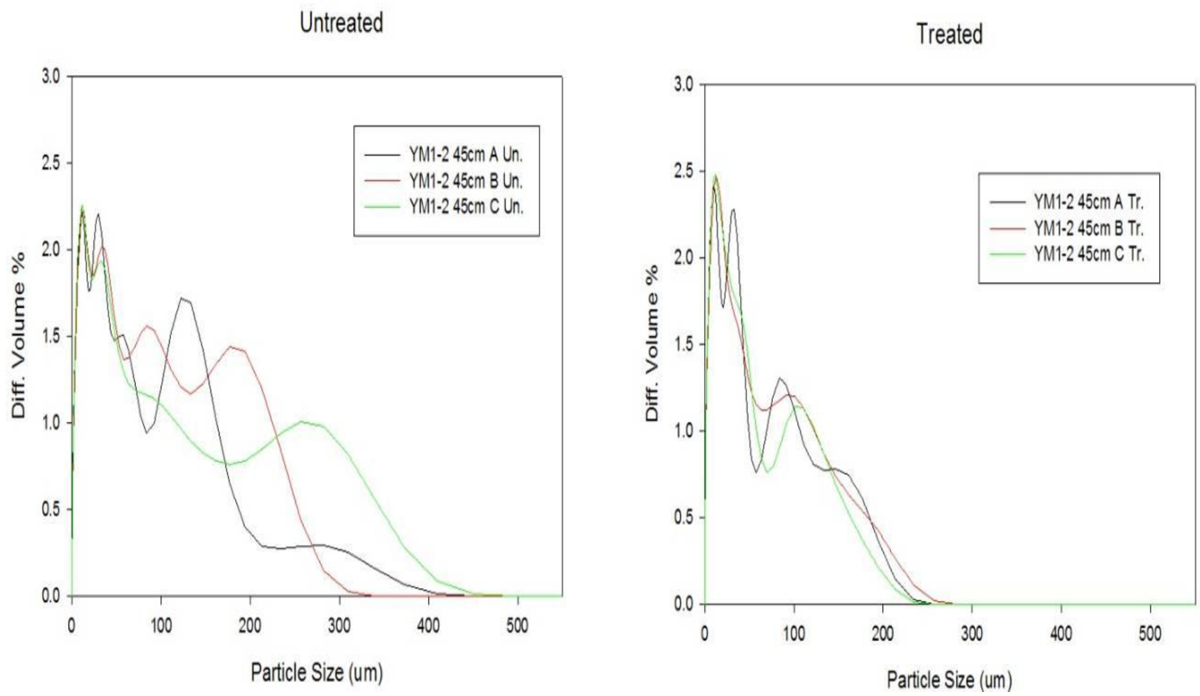

Figure 4.2 Graph of particle size distributions for YM-1-2 45cm determined for three subsamples of untreated sediment (left) and three subsamples treated with hydrogen peroxide (right). The subsamples treated with hydrogen peroxide are finer due to the removal of organic matter and the results are better replicated as shown above.

4.4 Separation, Quantification, and Characterization of the Low Density Fraction

In order to quantify the amount of discrete terrigenous organic matter in the event layers vs. the background sediments, the low density components (wood, seeds, charcoal, and non-woody debris) of the bulk sediments were removed by flotation in an aqueous solution of Sodium Polytungstate (SPT) with a density of 1.74 g/cm^3. To prepare the SPT, 140 gm of SPT powder was mixed with 100 ml of DI water in a clean, 1 L glass beaker. The water was stirred with a glass rod until all SPT powder had dissolved. The solution was passed through a 0.4 μm polycarbonate filter to remove any solid impurities. The density of the SPT solution was rechecked using a balance, and the solution was labeled and stored in a glass bottle.

Bulk sediments were thawed in their bags and homogenized using a metal spatula and then washed with DI water through a 63 μm sieve. Four to five grams of sieved sediment was placed into clean beakers and freeze dried overnight. Samples were removed from the freeze drier and ~1 g was placed into clean 15 ml polypropylene centrifuge tubes. Tubes were filled with SPT solution, shaken until the sediment was thoroughly mixed, and centrifuged for 30 minutes at 3000 rpm. The dense fraction, >1.74 g/cm^3, settled to the bottom while the low density fraction floated to the top.

A filtration apparatus was set up with a 0.45 μm polycarbonate filter membrane. The low density fraction from each centrifuge tube was decanted onto the filter and rinsed with 200-300 mL DI water to remove any remaining SPT solution. Once samples were thoroughly rinsed, the low density material was rinsed from the filters with DI water into clean petrie dishes. Samples were frozen, freeze dried, and covered with aluminum foil until further analysis.

The dried low density samples were examined under a polarizing microscope. Point counts of approximately 150 grains were made on each sample at 25x magnification. The total abundance of the different types of particles including pieces of wood, seeds, macro fauna, charcoal, and fly ash were quantified. Photos were also taken of representative samples from background sediments and event layers using Motic Images Plus 2.0 software.

4.5 Fourier Transform Infrared Spectroscopy – FTIR

Fourier transform infrared (FTIR) spectroscopy was used to provide a qualitative analysis of the minerals present in the millpond sediments. Samples were chosen from event layers and background sediments in an attempt to detect differences in their mineralogy. Unlike x-ray diffraction, FTIR allows for the identification of both crystalline and poorly crystalline minerals (Farmer and Russel, 1967) with a quick turnaround time. FTIR uses infrared radiation to produce lattice vibrations between bonded atoms within the mineral, including stretching and bending vibrations. Minerals absorb infrared radiation at different energies and produce unique absorption peaks, which can be used for identification.

To prepare a sample for FTIR, it is suspended in matrix of KBr. Since KBr is transparent to IR, it does not interfere with the absorbance spectrum. Spatulas, mortar and pestle, and dies used for FTIR are stored in a blower oven at 70°C, along with the KBr powder, due to its hygroscopic nature and the adverse impacts water can have on analysis. One to two grams of the <63 μm sediment fraction was freeze dried overnight to remove any excess moisture from the sample. Approximately 0.5 mg of sample and 80 mg of KBr powder were weighed and then ground in an agate mortar into a well homogenized fine powder. This powder was then carefully transferred to a die using a clean spatula and tapped down until a flat surface was obtained. The disc was placed into a hand press and pressure was applied until a transparent wafer had formed.

Infrared spectra were obtained using a Nicolet Impact 400D FTIR spectrometer which has a detectable range of 4000-400 cm^{-1}. Spectra were collected using the Omnic software package, and peaks were analyzed using PeakFit v4.12 (Systat Software Inc.). A constant baseline with a tolerance of 3.0% was subtracted from each spectrum, and peaks were identified using the Voigt Area G/L function after smoothing using the Loess function. Mineral identifications were made based on comparisons to published spectra compiled by Katherine Almquist (Almquist, 2010), whose characteristic peaks are given in Table 4.1.

Table 4.1 Key peaks used in identifying minerals in FTIR.

Mineral	Peak Positions (cm^{-1})
Montmorillonite	426-430, 465-467, 520-525, 675, 770, 815-818, 830-845, 890, 915-917, 1026-1040, 1090, 3420-3426, 3556, 3620-3624
Water, especially in Montmorillonite	1630
Kaolinite	430-432, 470-472, 539-540, 912-913, 938, 1005-1011, 1031-1032, 1100, 3619-3622, 3695-3696
Kaolinite, Illite	750-753
Kaolinite, Illite, Montmorillonite	690-695
Kaolinite, Halloysite	795
Quartz	512, 778-780, 798-799
Biotite	646, 1000, 3590
Biotite, Montmorillonite	1108-1115
Biotite, Montmorillonite, Muscovite	1165-1170
Chlorite	660, 3434, 3485, 3560-3570, 3627
Chlorite, Illite	985-990
Chlorite, Illite, Quartz	1080-1085
Calcite, Dolomite	875-880, 1420-1430
Albite	400, 700-800 quartet
Halloysite	650, 692, 941, 1012, 1094
Illite	825
Anorthite	929
Imogolite	993
Allophane	1016, 3300
Vermiculite	3571

Compiled by Almquist, 2010, from the following references: Russell, 1987; Russell et al., 1981; Wilson, 1994; Madejová and Komadel, 2001; Ohashi et al., 2002; Post and Borer, 2002; Pironon et al., 2003; Certini et al., 2006; Van der Marel and Beutelspacher, 1976

4.6 Sediment Dating Techniques

4.6.1 ^{210}Pb Analysis

Bulk sediments were selected from Yates Mill (core YM-1) and Mitchell Mill (core MMP-2) for determining ^{210}Pb sediment accumulation rates. After drying, sand was removed and Po-209 spike solution, the granddaughter to ^{210}Pb was added, which is alpha-emitting and actually provides more accurate estimates of ^{210}Pb than will direct measurements (Jeter, 2000). Dried sediments were leached in 80°C HCl and also treated with hot HNO_3 to remove the organic matter. After this treatment, the solution was evaporated to dryness. Nitric Acid (which can interfere with plating) was completely replaced with hydrochloric acid after dissolution and the evaporation cycle was repeated at least three times. The solution was centrifuged three more times using HCl and the liquid solution was then used for plating the dissolved Po-209 onto a silver planchet. Ascorbic acid was added to the solution to complex any remaining iron, and polished silver planchets were allowed to plate overnight (methods from Dr. Dave J. Demaster; used in Demaster et al, 1994).

Total ^{210}Pb activities were determined by counting alpha emissions for at least 48 hours. ^{210}Pb activity was then calculated using the results as shown:

$$^{210}\text{Pb Total Activity} = \frac{(\text{209 Po Spike})(\text{Counts 209 Pb} - \text{BGD})}{e^{-\lambda \Delta t}\,(\text{Counts 209 Pb} - \text{BGD})(\text{weight of sample})}$$

^{209}Po Spike = 57 dpm (during testing period)

$$\text{BGD (Background)} = \frac{\text{Background Counts}}{\text{Background } \Delta t} \text{ x Counting period for sample}$$

λ = ln 2 / half life of ^{210}Po (138 days)

Lead-210 is a naturally occurring radioactive element that is found in small quantities in most soils as part of the uranium-238 radioactive decay series. It is also produced by natural fallout (rain and dust) from the atmosphere through the decay of radon-222 gas. ^{210}Pb mixes and sorbs onto sediments which accumulate at the bottom of water bodies. Within two years ^{210}Po, the granddaughter of ^{210}Pb, is in secular equilibrium with ^{210}Pb, and as previously mentioned, it is this alpha emitting ^{210}Po which is measured. Due to radioactive decay, this "excess" ^{210}Pb is generally detectable only in sediments deposited in the past 100 years. At depths corresponding to 100 years and older, the excess ^{210}Pb has decayed away and the only remaining ^{210}Pb is that produced by *in situ*, or "supported" decay of radiogenic uranium contained in mineral grains (Jeter, 2000). Excess ^{210}Pb values were determined by subtracting supported levels of activity from total ^{210}Pb activities. The natural logs of excess ^{210}Pb activities were then plotted against the depth in the core and a regression line was fit through the data points. The apparent accumulation rate was determined by dividing the decay rate of ^{210}Pb by the slope of the regression line (methods adapted from Haskin, 1972). The rate determined is a maximum possible rate based on the assumption that the profile has not been affected by biological mixing (bioturbation).

4.6.2 Dendrochronology

The use of tree ring chronologies (dendrochronology) to date geomorphic events has been well established (Heikkinen, 1994; Wiles et al., 1996; Speer, 2010). Its applicability in dating the top of the millpond deposits was investigated at Cook's Millpond. Since the oldest trees on the relic millpond floor can be no younger than the draining of the pond, assumed to be the first succession of growth on an exposed millpond bottom (given that there have been no disturbances to the tree stand), their ages should be very close to the time of dam breaching.

The tree stand history at the Cook's Mill site is relatively well documented. The landowner of the site when the dam breached, near 1910, cleared the landscape to the northwest of the pond. The cleared land surface, shown on historical photos in 1938 and 1959 (USDA Farm Service Agency) appears to be lighter in color, while the area near the dam, surrounding the stream appears to be darker in color indicating it was forested (Figure 4.3).

An increment borer was used to extract cores from living trees for analysis of maximum age (methods described in Grissino-Mayer, 2003). At Cook's Millpond, the largest trees available for coring were deciduous hardwoods, namely oak, maple and birch. Two cores, parallel to one another on opposite sides of the tree, were taken from each tree for an estimate of overall tree growth chronology (Clark et al., 2004; Speer, 2010).

During the months of October-December 2011, a total of 24 cores were taken from 12 trees. Cores were stored in vented plastic straws and later mounted on a wooden sample holder. Each core was cut lengthwise parallel to the sample holder surface and sanded with 100 to 400 grit sandpaper. They were then visually analyzed under a binocular microscope at 30x magnification and the width of individual rings measured and recorded with a Velamex Rapid Advance Unislide linear encoder that interfaces between the microscope and a PC (Speer, 2010). This process starts by assigning the year of the core acquisition to the bark end of the sample and then counts rings backwards in time to the sample pith. Total ring widths (including early and late wood) were measured to within 0.01 mm using the MeasureJ2X software package interfaced to the Velamax encoder. When a core missed the pith, a pith indicator was used to estimate the age (Applequist, 1958). A pith indicator is a series of concentric circles, which when matched to the curvature of the tree's rings can give an accurate estimate of the number of rings missing.

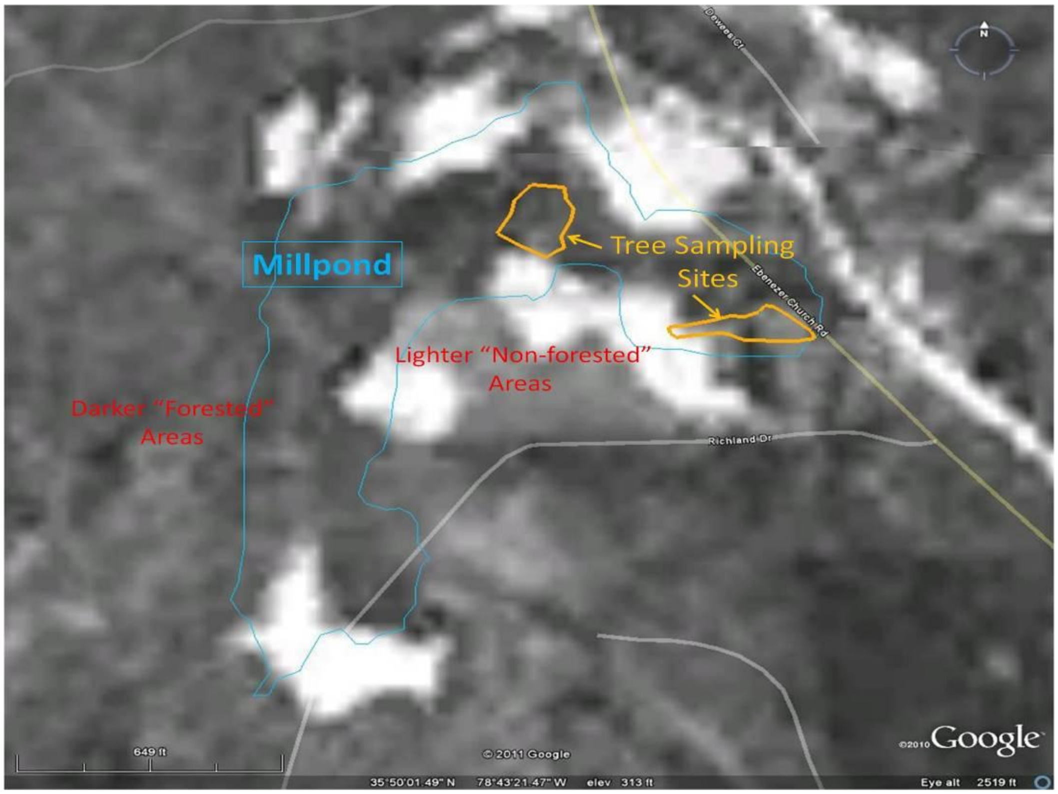

Figure 4.3 Google Earth image (2010) of tree core locations at Cook's Mill with a 1938 aerial photo (USDA Farm Service Agency) overlay showing forested (dark grey areas) and non-forested (lightly colored) areas.

5.0 RESULTS

5.1 ArcGIS Mapping

The results of Arc Map analysis of the original extent of the millponds are shown in Table 5.1 and in Figures 5.1-5.5. Of the five studied ponds, Betty's Mill was the smallest at 0.025 km^2, and JD Hayes is the largest at 0.17 km^2. Over time, sediment has accumulated at these sites reducing water storage capacity, for example, Mitchell Mill has been reduced from an original area of 0.037 km^2 down to 0.009 km^2, while the perimeter of the pond has remained relatively constant (Figure 5.5).

Using terrain analysis, slopes were calculated for all input streams at each of the mill sites (Table 5.2). Results show that the slopes of all the streams are relatively low, with an average gradient of 0.0076. Typical longitudinal pond profiles, created using elevation values from the DEM, drawn from the inlet stream(s) to the dam show that the pond bottom is asymmetric, with the more gently sloping bottom at the upstream end suggesting the outbuilding of a delta (Figure 5.6). A profile across the width of the former pond site at Cook's Mill shows the incision of the stream into the flat pond sediments (Figure 5.7).

Umstead Park, NC Millpond Sites

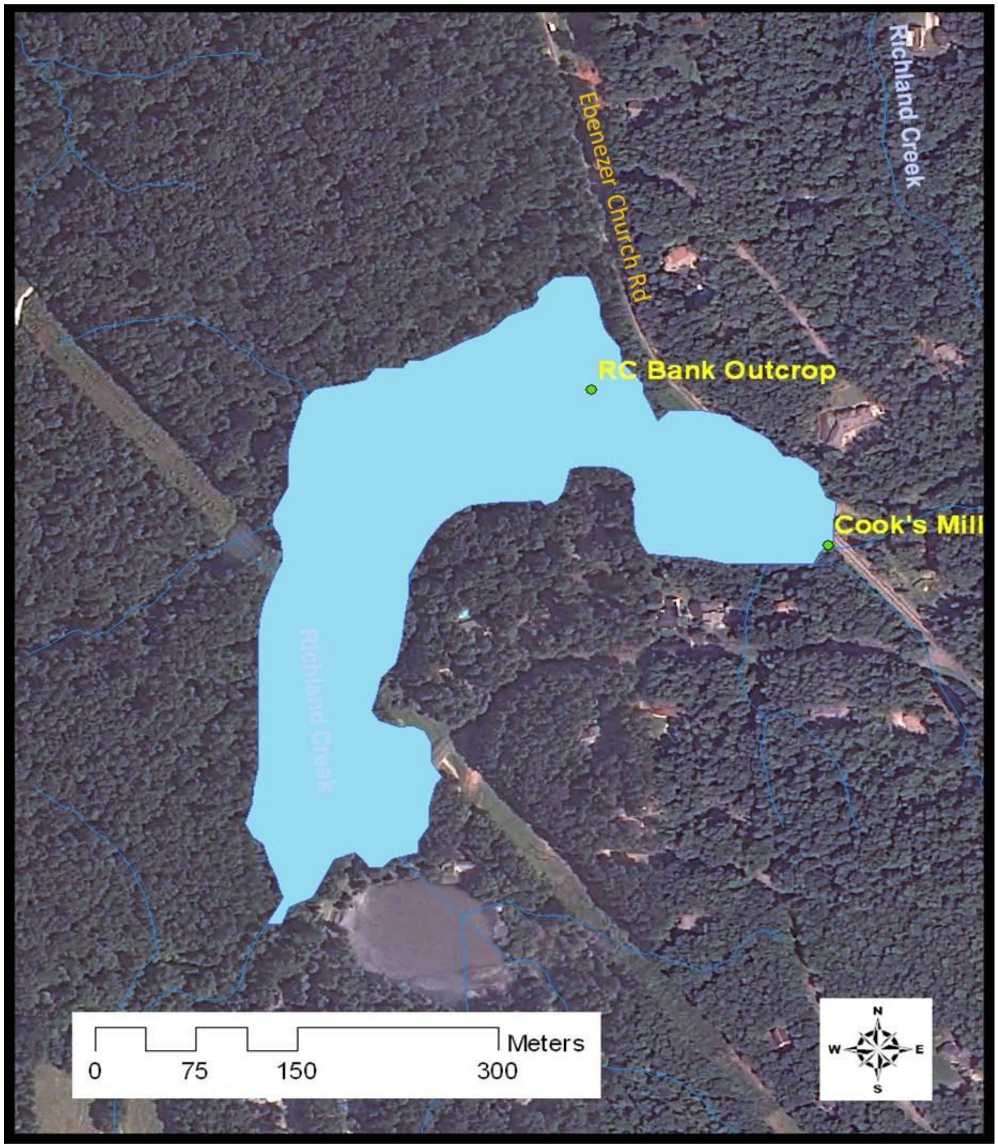

Figure 5.1 Digitized surface of relic pond at Cook’s Mill.

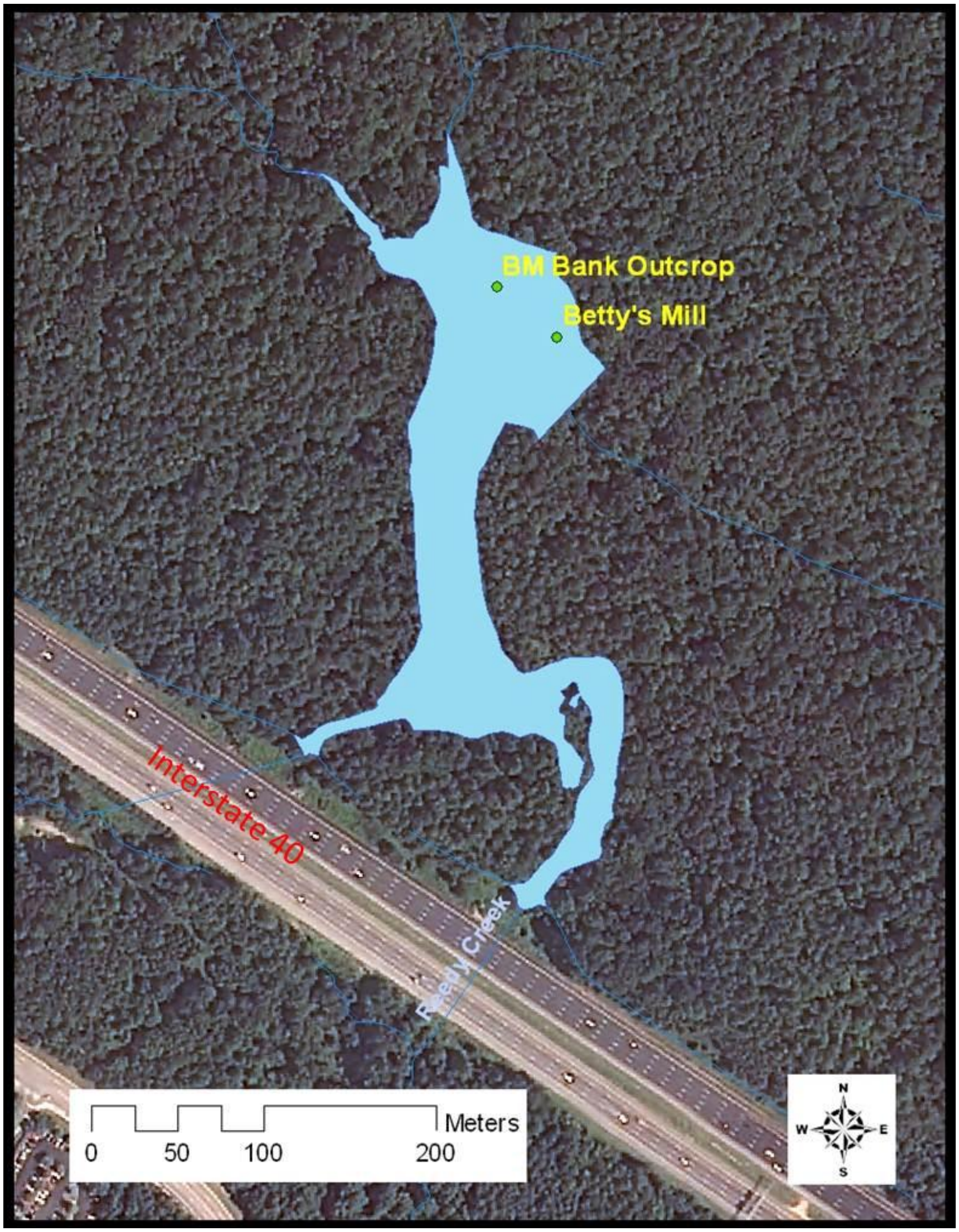

Figure 5.2 Digitized surface of relic pond at Betty's Mill.

Raleigh, NC Millpond Sites

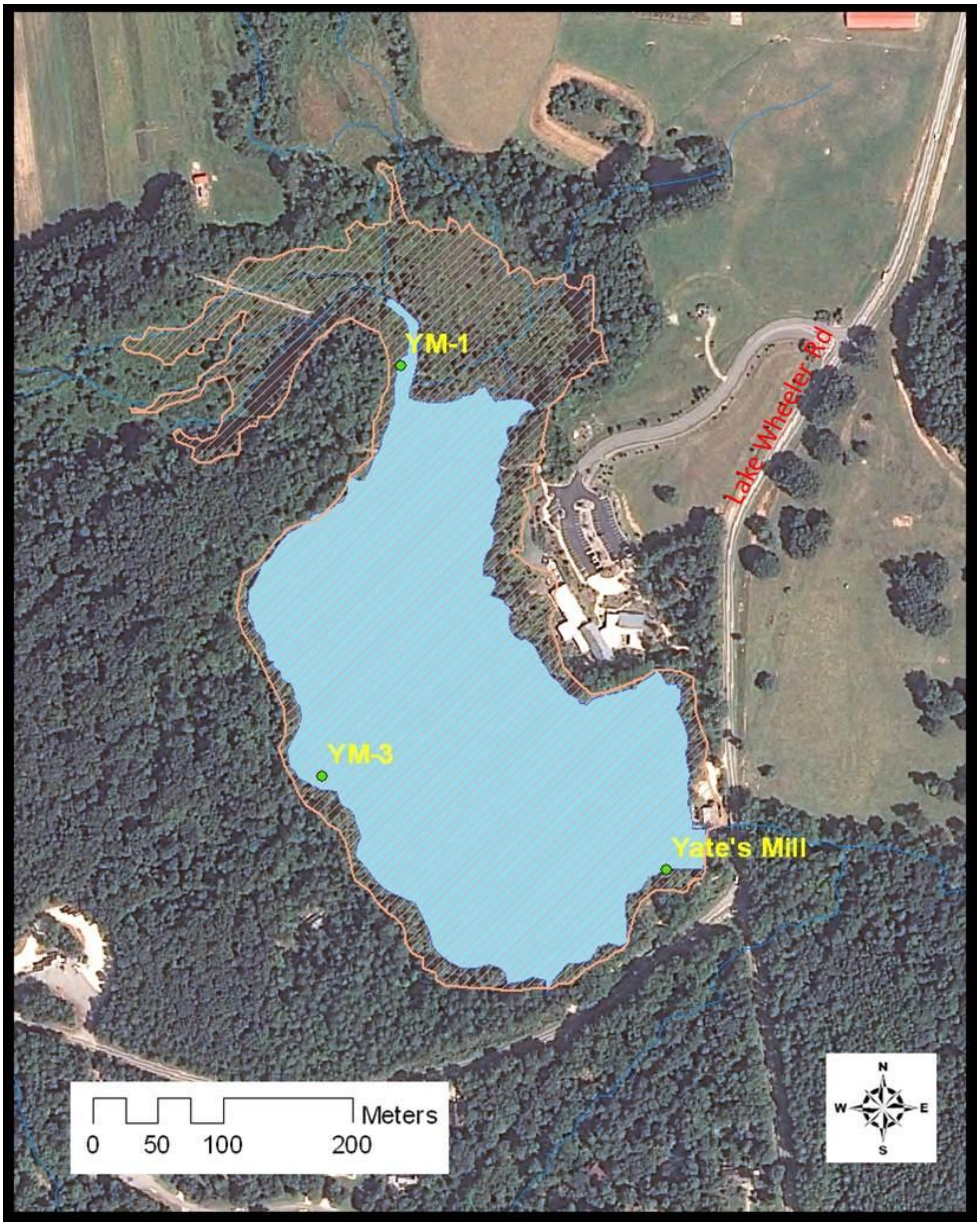

Figure 5.3 Yates' Mill with current millpond surface (light blue) and relic surface (orange).

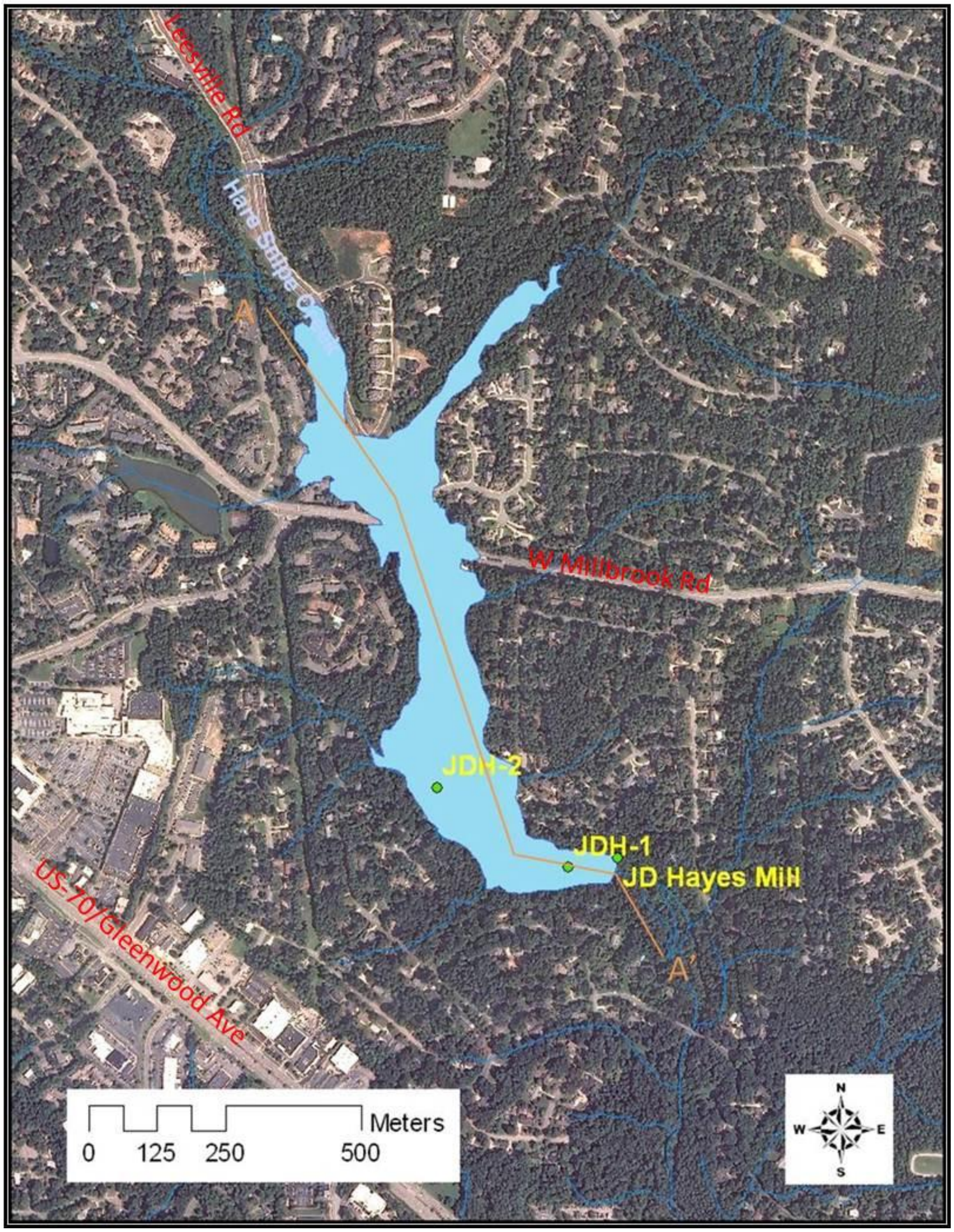

Figure 5.4 Digitized surface of relic millpond at JD Hayes.

Figure 5.5 Mitchell Millpond with current millpond surface (light blue) and relic surface (orange).

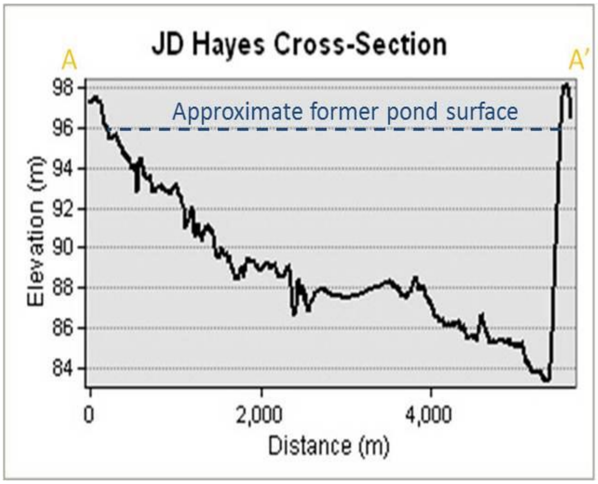

Figure 5.6 Profile of the relic JD Hayes Millpond from the inlet stream to the location of the dam remains.

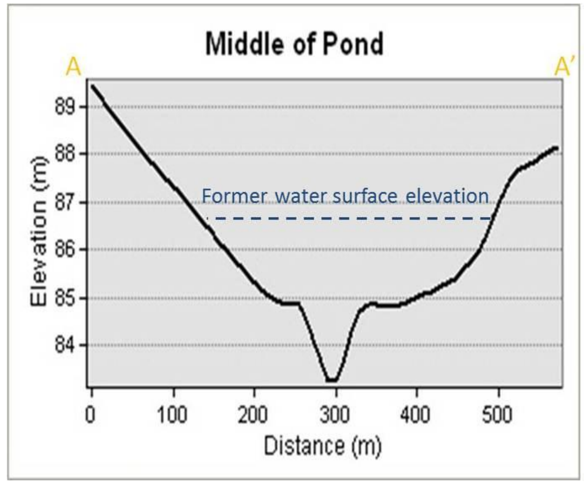

Figure 5.7 Profile across the middle of the Mitchell Millpond showing incised stream channel.

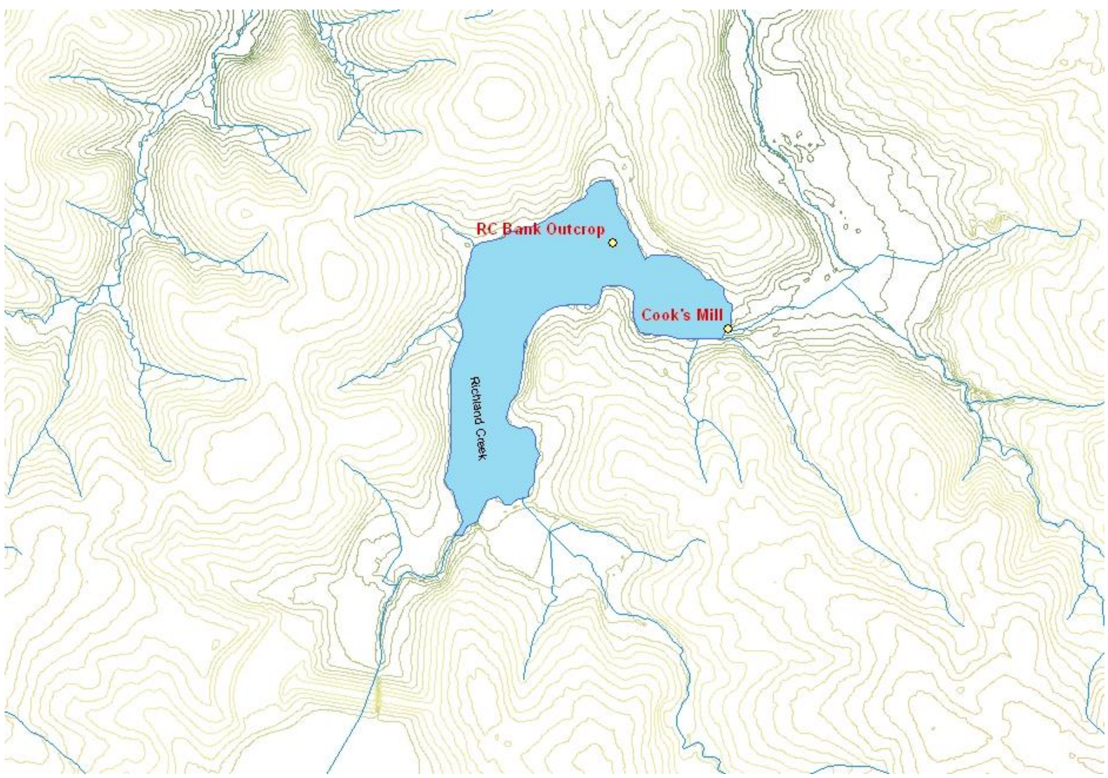

Figure 5.8 Topographic map of the former millpond at Cook's Mill site.

Table 5.1 ArcGIS generated results showing spatial values for all mill sites studied.

Stream	Mill_Name	Dam Height (m)	Perimeter (m)	Area (m^2)	Acres	Hectares
Reedy	Betty's	4.2	1702	25095	6.2	2.5
Hare Snipe Creek	JD Hayes	3.8	4348	173624	42.9	17.4
Richland Creek	Cook's	6.1	1917	84007	20.8	8.4
Swift Creek	Yate's (Current)	4.9	1736	90649	22.4	9.1
Swift Creek	Yate's Relic Pond		2851	139803	34.6	14.0
Little River	Mitchell (Current)	2.8	1107	8775	2.2	0.9
Little River	Mitchell Relic Pond		1159	36508	9.0	3.7

Table 5.2 Calculated slopes of the streams which discharge water/sediment into the millponds of interest.

Site	Upstream Elevation (m)	Downstream Elevation (m)	Distance (m)	Slope
Betty's Mill	106	92	1720	0.008
Cook's Mill (A)	97	86	2440	0.005
Cook's Mill (B)	129	88	2880	0.01
JD Hayes' Mill	137	89	5590	0.009
Yates Mill (A)	133	90	6610	0.007
Yates Mill (B)	137	89	4480	0.01
Mitchell Mill (A)	98	85	3270	0.004
Mitchell Mill (B)	97	84	3190	0.004

5.2 Stratigraphy and Grain Size Analysis

Identification of the stratigraphic facies was done using comparative interpretations from Walter and Merrits, 2008. As shown in Figure 5.9, depositional environments for each sedimentary layer encountered in the millpond profiles were interpreted using Walter and Merrits descriptions as: I) Gravel-rich stream deposits, II) Wetland soils prior to colonization, IV) Millpond sediments. However, it was found that one additional layer below the mill deposits had to be accounted for in the Wake County records, layer III, Channel Fill (pre-dam legacy sediment). This layer is interpreted to record aggradation of the streams after colonization, when the land was being cleared, but before construction of the local milldam (Lewis, 2011).

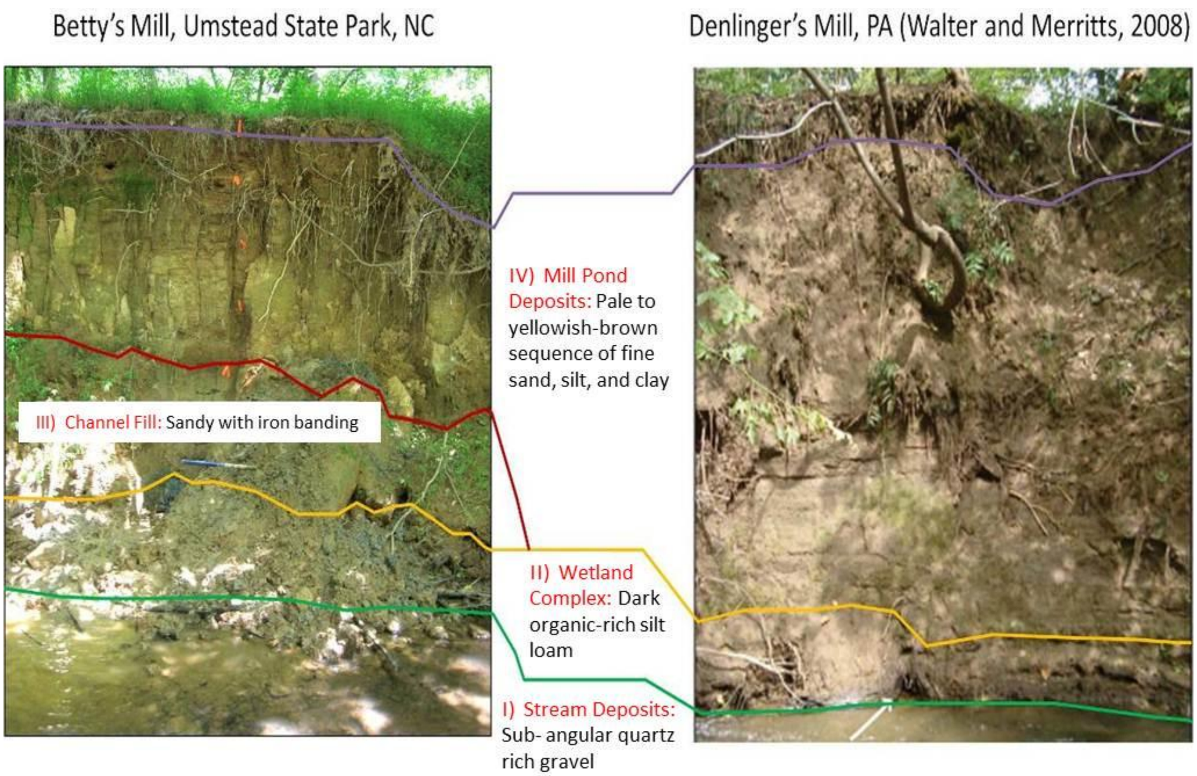

Figure 5.9 Comparison of the stratigraphy found at Betty's Mill, NC and Delinger's Mill, PA (Walter and Merrits, 2008).

5.2.1 Cook's Mill

At the base of the profile (-78.72218 long., 35.83532 lat.) is a facies consisting of quartz-rich pebbles and cobbles (I), which is overlain by wetland soil that is 34 cm thick and fines upwards. Above the wetland facies is the channel fill facies, which is 103 cm thick and is composed of interstratified coarse and fine deposits interpreted to record a series of channel migrations throughout time (Schumm, 1981). The channel fill sediments (III) and wetland soil (II) are much coarser than the overlying facies, with a mean grain size of 227µm (silty sand) and 288 µm (sand) respectively. The millpond deposits (IV) are 183 cm thick, and are composed of fine-grained sediments with interstratified, thin sandy event layers. The event layers both coarsen and thicken upward through the millpond profile. The results of grain size analysis at the Cook's Mill site are shown in Figure 5.10. Ten discrete sand layers were initially recognized in the profile. Particle size analysis of subsamples from the thickest layer (4 cm thick) were taken at equal 3 mm intervals, and suggest that it is composed of two amalgamated, graded layers (Figure 5.11). The mean grain size (D_{50}) of the sandy event layers is 129 ± 83 µm (fine sand), while the interstratified finer-grained deposits average 20 ± 4 µm (silt).

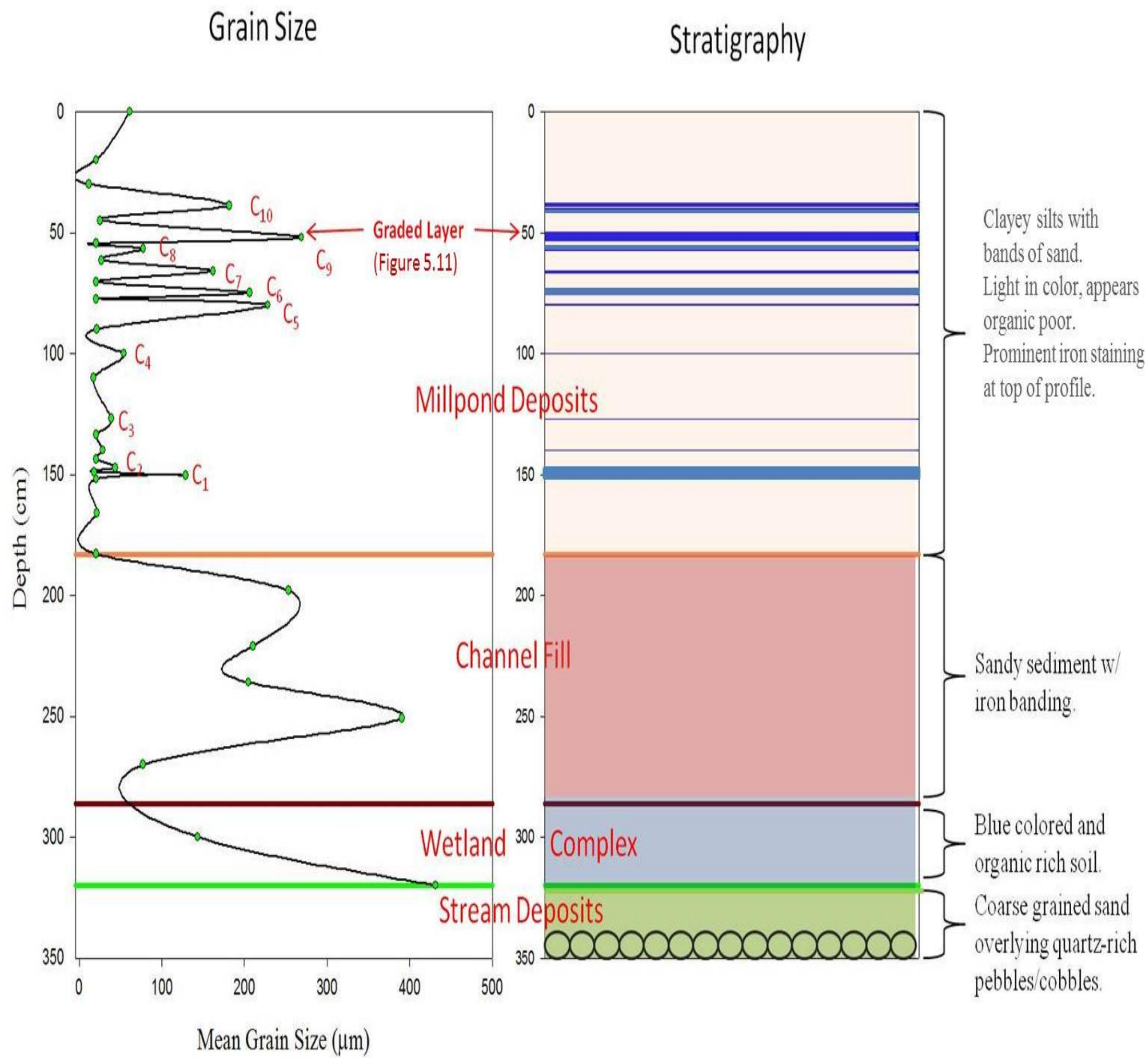

Figure 5.10 Mean grain size for Cook's Millpond with sand layers C_1-C_{10} (on left) and observed stratigraphy at bank outcrop (on right) (Figure 5.1).

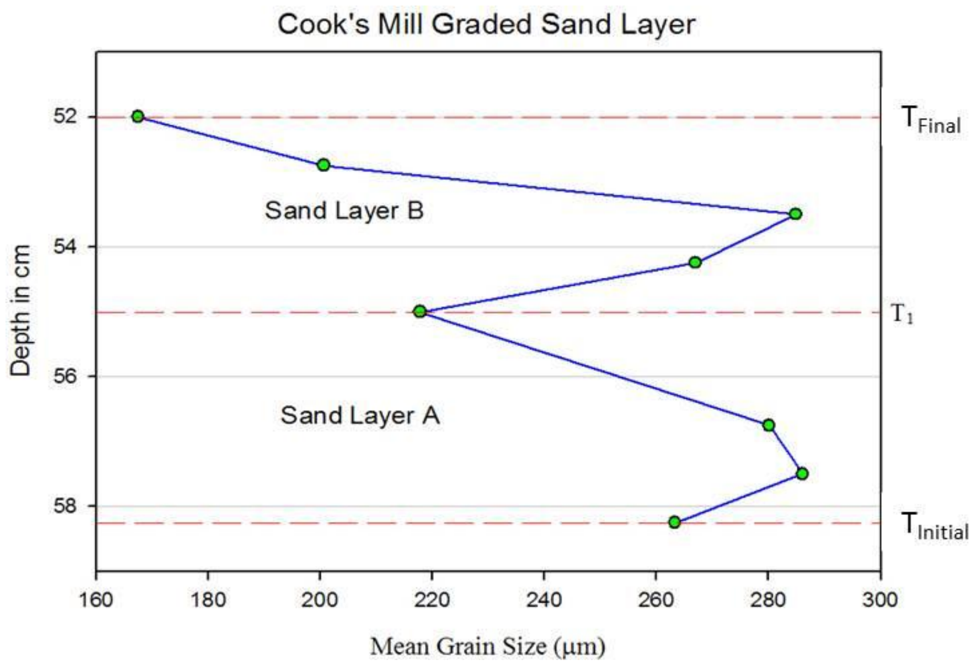

Figure 5.11 Four-centimeter- thick graded layer shown in Figure 5.10, interpreted to record two storm events or two pulses of precipitation/high river discharge during a single event.

5.2.2 Betty's Mill

The stratigraphy at Betty's Mill (-78.753575 long., 35.829708 lat.) is similar to that exposed at Cook's Mill based upon the interpretations shown in Figure 5.10. Field observations show that the wetland facies at the base of the stratigraphy (Figure 5.12) do not exhibit as much blue staining (gleying) as at Cook's Mill. It was also observed that of the sand layers investigated, only S_3 contained gravel sized pebbles at its base. The thicknesses of each facies are as follows: the stream deposits are approximately 30 cm thick, the wetland facies is 20 cm, the channel fill facies are 55 cm, and the millpond sediments are 205 cm.

The millpond sediments at the Betty's Mill site contain a larger number of coarse layers than do those at Cook's Mill (23 vs. 10), but many of these are millimeter scale in thickness and therefore cannot be sampled accurately. Five samples were taken in total, three of which were from the thickest sand layers, sand layer 1 (S_1) = 4 cm, sand layer 2 (S_2) = 5 cm, and sand layer 3 (S_3) = 3 cm thick (Figure 5.12). The grain sizes of the sand layers was S_1 = 421 µm, S_2 = 587 µm, S_3 = 699 µm, with a mean of 569 µm (medium sand). Two fine-grained background samples were also collected, one at 193 cm in depth, and the second at 30 cm in depth. Their grain sizes were 13 µm and 126 µm respectively, indicating that the sediments are coarsening upwards through the profile.

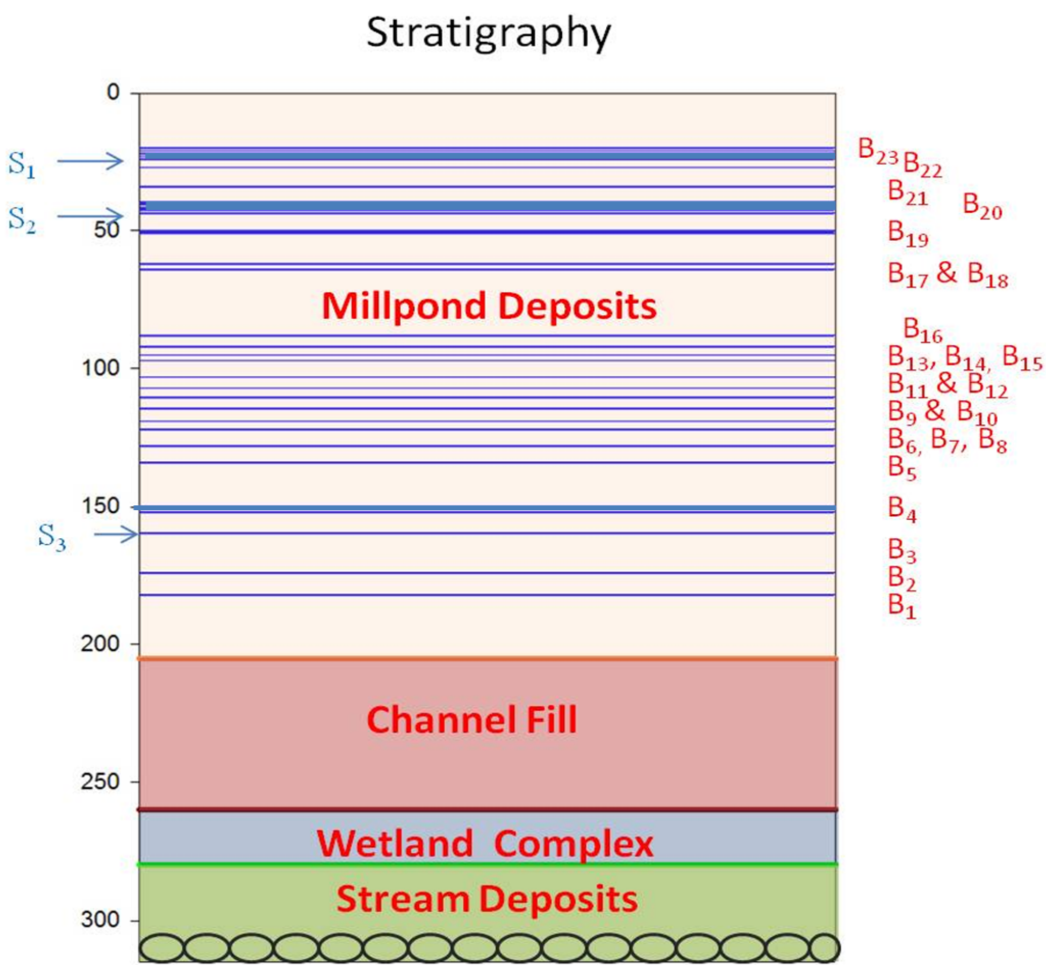

Figure 5.12 Stratigraphic profile through the Betty's Millpond sediments with observed sand layers B_1-B_{23} noted (Figure 5.2), and the locations of collected samples indicated (S_1-S_3).

5.2.3 Yates Mill

YM-1:

Taken at the upstream end of the Yates Millpond (Figure 5.3), core YM-1 (-78.688931 long., 35.721403 lat.), was 99 cm thick, and revealed 9 possible event layers. The core barrel was hammered into the borehole until the bit came into contact with coarser stream deposits (small gravel was removed from the bottom of the core), which bent the auger head. The core is composed of clayey silt with interstratified sand layers, and there is a downward fining trend from the surface to the top of the thick and coarse layer at the core bottom (Figure 5.13). Woody debris is abundant throughout the profile.

YM-3:

YM-3 (-78.689608 long., 35.718453 lat.) was recovered approximately 10 meters from the western bank of the current millpond (Figure 5.3). The core barrel was hammered into the soft millpond sediments until coarser deposits were encountered. The total length of the core was 83 cm. At 35 cm depth, there is a sharp transition between relatively fine-grained sediments to much coarser, well stratified deposits (Figure 5.13). At this same depth, the sediments transition from a dark grey color (5Y 5/1) to a reddish yellow (5YR 5/4) color (Munsell Color Chart). The background sediments are much finer than in YM-1, and are composed of clayey silt. At the base of the core, the sediments are characterized by blue gray, silty clay, suggesting accumulation in a reducing environment.

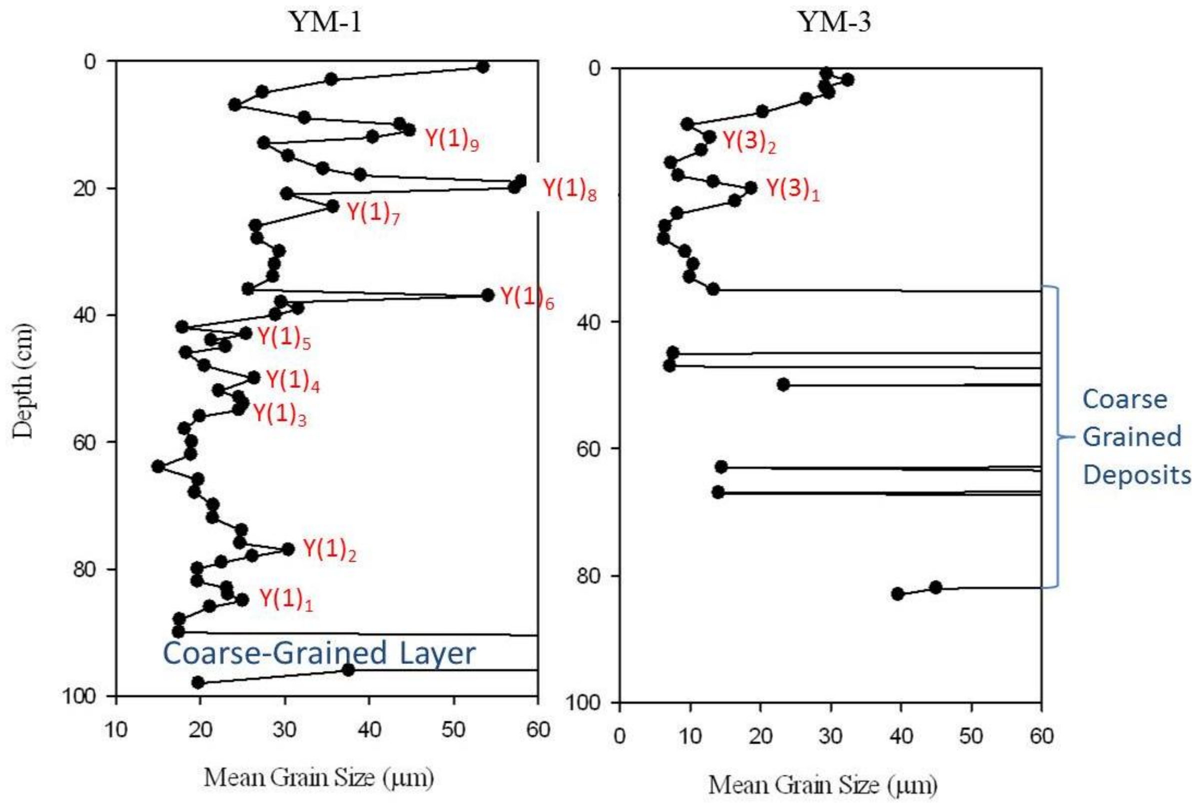

Figure 5.13 Mean grain size of sediments from two cores (Figure 5.3) taken at Yates Mill Pond. Coarse layers, possibly the result of storm events, are labeled.

5.2.4 JD Hayes Mill

<u>JDH-1</u>:

Core JDH-1 (-78.69244 long., 35.85675 lat.) was recovered from the exposed and vegetated relic millpond surface, relatively close to ruins of the dam at the JD Hayes site (Figure 5.4). In the field, when the core was driven into the ground, the auger tip was badly damaged due to contact with bedrock, and rock fragments were found in the core catcher. The coarse, sandy texture of the sediments in this core suggest deposition very near the pond shoreline or in a shallow area of the pond dominated by sediment bypass, and it was not used further to reconstruct storm history.

JDH-2:

JDH-2 (-78.69511 long., 35.85809 lat.) was retrieved in two segments which totaled 107 cm from a site much further upstream of the dam than JDH-1, in the middle of the relic millpond (Figure 5.4). Sediments in the core were finer than those in JDH-1 with a small amount of visible organic remains (i.e. wood fragments, leaves, etc.), and also exhibited a coarsening downward trend. Sediments in the upper portion of the core are finer than those below and as such are the only suitable portion of the core for the identification of possible sandy event layers.

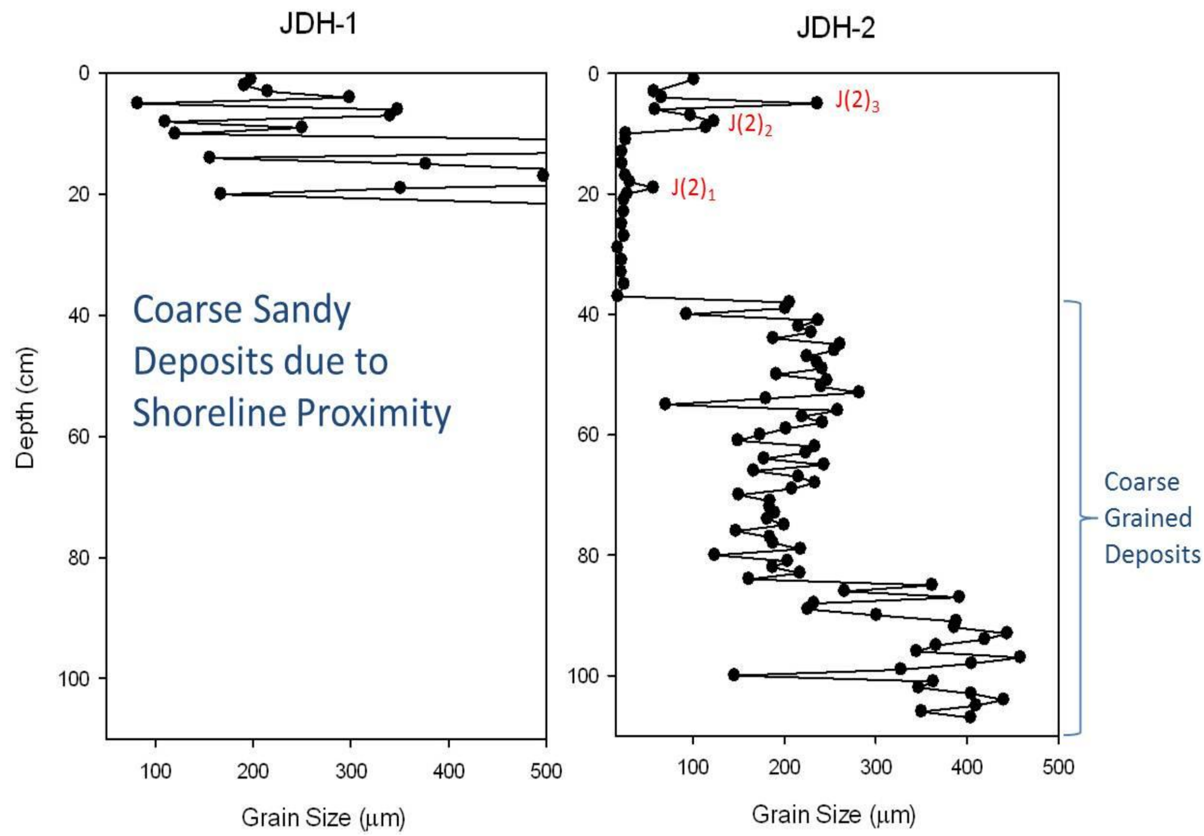

Figure 5.14 Trends in mean grain size in two cores recovered from the site of JD Hayes Mill Pond (Figure 5.4). Interstratified sandy layers are numbered from the bottom of the cores.

5.2.5 Mitchell Mill

<u>MMP-1</u>:

MMP-1 (-78.38834 long., 35.9147 lat.) was cored approximately 50 m upstream of the dam near the right bank (looking downstream) of the main stream channel (Figure 5.5). Like JDH-1, which was also recovered near the stream channel, the core was relatively short in length, 33 cm. Seven coarse sand layers are interstratified with fine silt in this core. The sandy event layers are fairly evenly spaced, but are notably absent between 23 and 29 cm in the core.

MMP-2:

MMP-2 (-78.38763 long., 35.91502 lat.) was recovered in a wetland environment in an area of the relic millpond that is now closed off from the main channel by a vegetated island (Figure 5.5). MMP-2 consisted of two core segments with a total length of 111 cm. The core is composed of mostly fine-grained clayey silt that coarsens slightly upward in the core. Plant remains are especially abundant around 20-30 cm below the surface. Eleven thin, coarse sand layers are interstratified with the fine grained sediments.

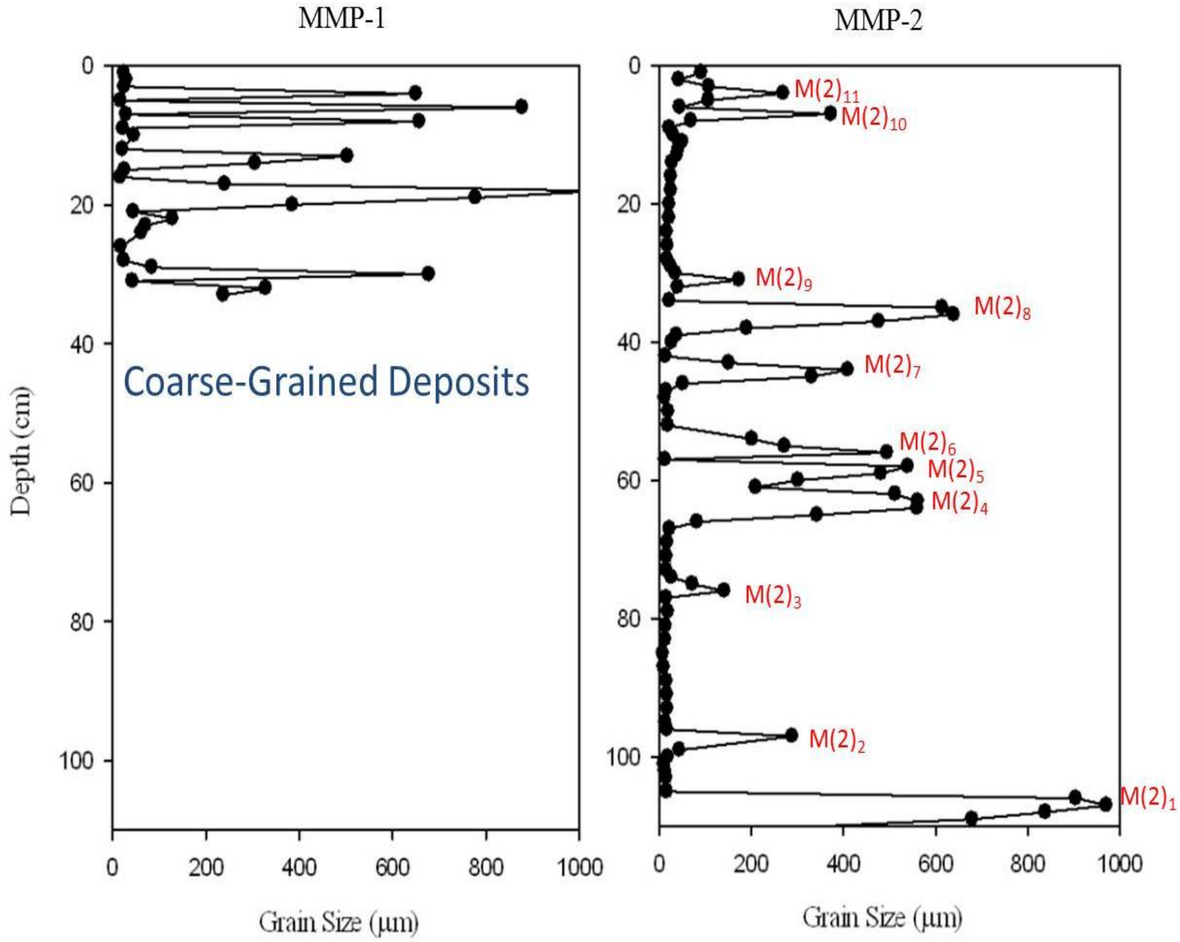

Figure 5.15 Trends in mean grain size in two cores (Figure 5.5) recovered from Mitchell Mill Pond.

5.3 Point counts of low density material

Point count data are presented in terms of the proportion of various constituents in the low density material isolated from each sample. Seed content shows no discernable variation, with seeds accounting for about 3 % of the low density material in both the event layers and background sediments. Small non-woody debris, including algal cysts was present in low concentrations in both background sediments (4%) and in the sandy event layers (1%). The low density fraction of background sediments contained more fly ash than did the event layers, 10% vs. 4% (Figure 5.16).

Event layers and fine-grained background sediments differed in their wood and charcoal content. Wood fragments were a larger proportion of the low density material in many of the event layers, and generally a much lower proportion in the background sediments (Figure 5.17). The opposite was true with charcoal, which was relatively less common in the event layers (43% of the low density material), than in the background sediments (65% of the low density fraction) (Figure 5.16).

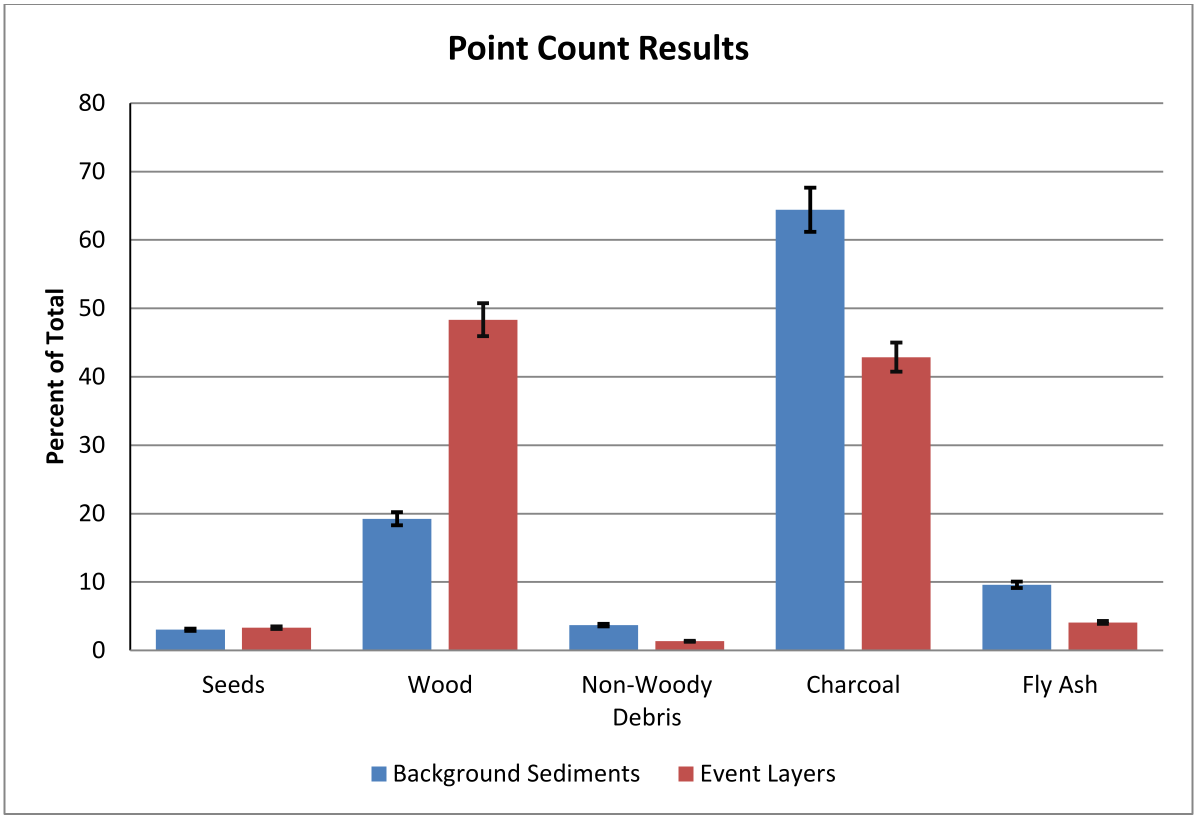

Figure 5.16 Estimates of the composition low density material in event layers vs. background sediments based on point counts with 5% standard error bars. Categories were seeds, woody debris, non-woody debris (including algal cysts), charcoal, and fly ash. Event layers contain much more wood than do background sediments.

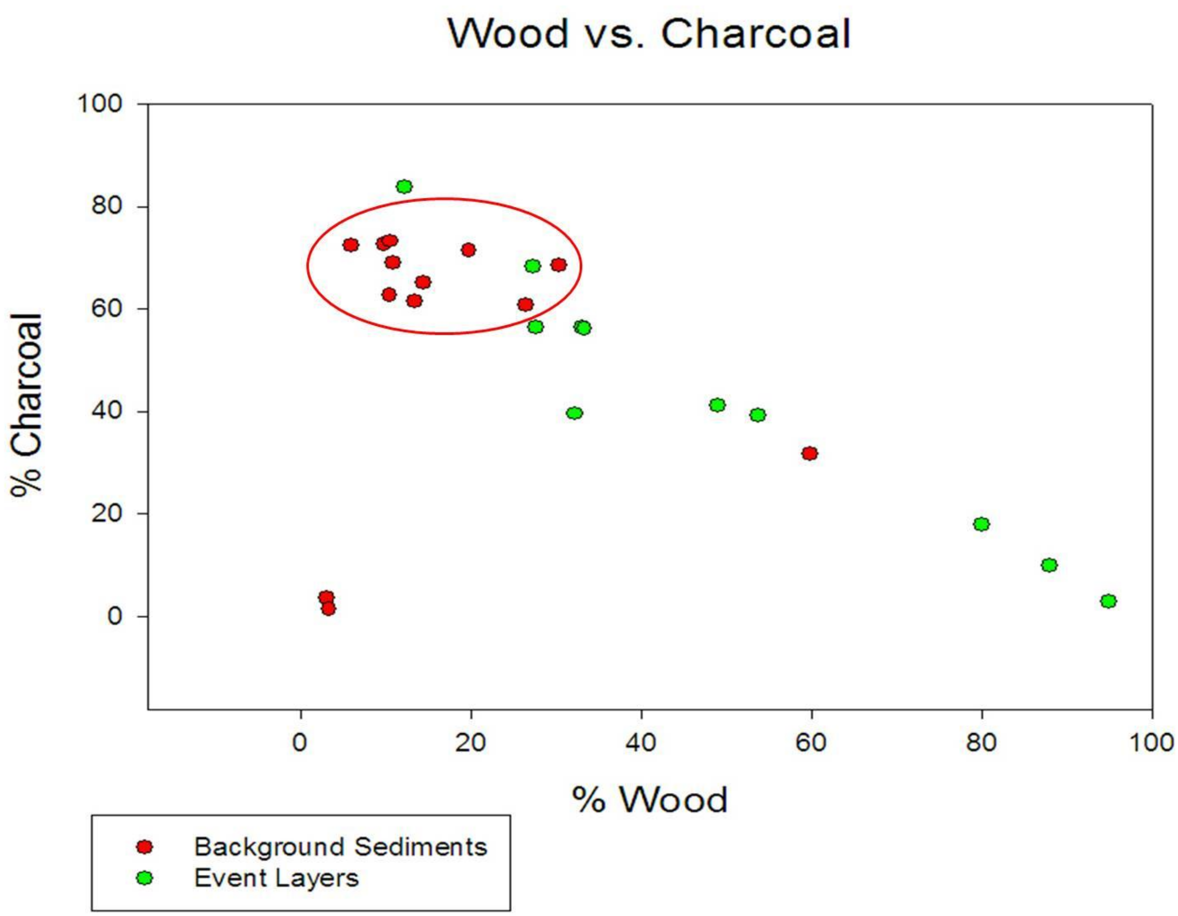

Figure 5.17 Graph of % wood vs. % charcoal. Background sediments are typically low in wood content, but high in charcoal. The amount of charcoal and wood is variable in the event layers.

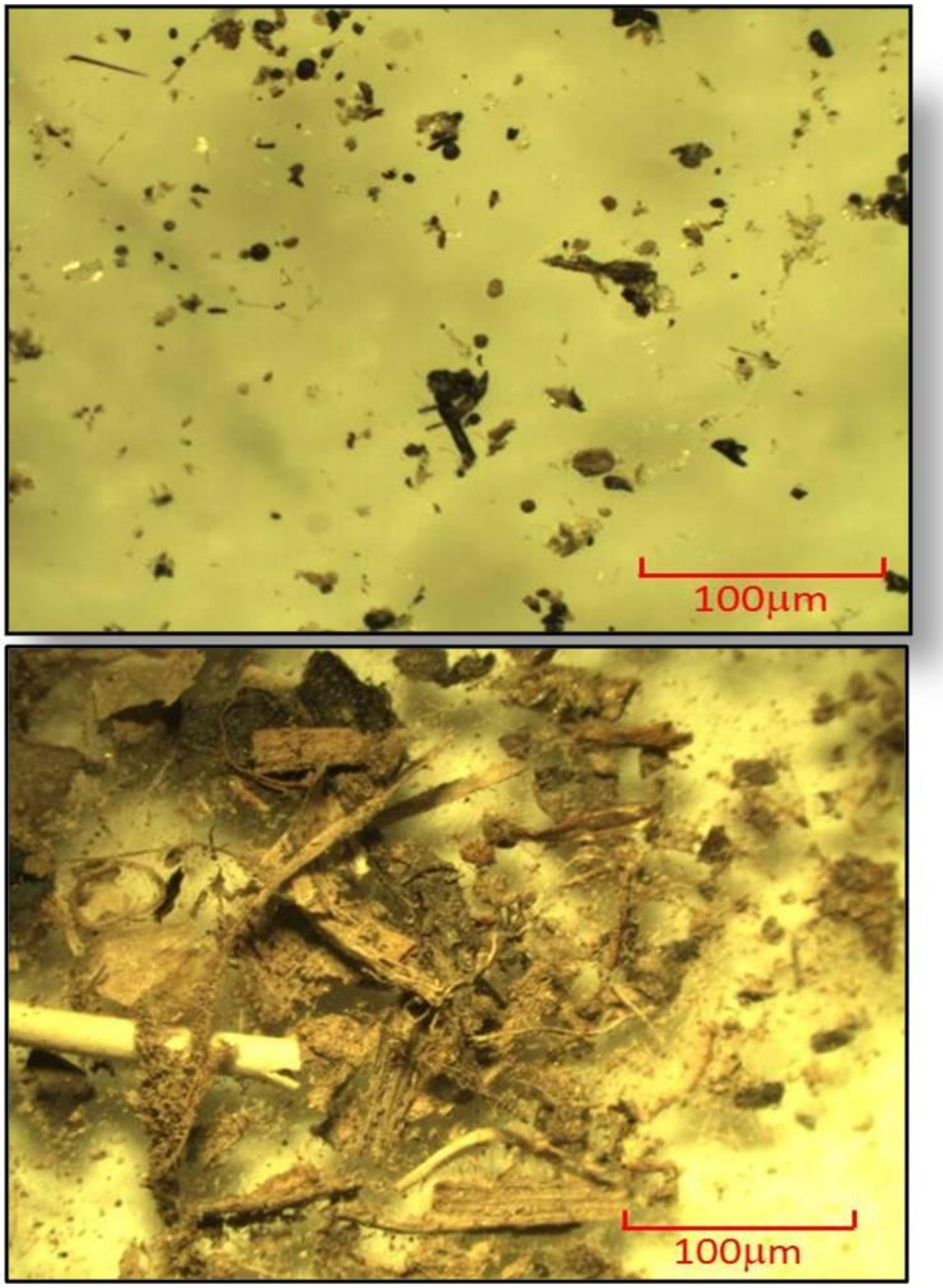

Figure 5.18 Photomicrographs of representative low density components from background and sandy event layers. Top: low density fraction from background sediments in YM-1-1, 17 cm in depth; Bottom: low density fraction from an event layer in MMP-2-1, 49 cm in depth. Notice the amount of large woody debris in the event layer, which is a rare component of the low density fraction in background sediments.

5.4 Fourier Transform Infrared Spectroscopy – FTIR

FTIR was performed on a total of 21 samples, 10 background sediments and 11 event layers. After the peak locations were determined with the help of the PeakFit software, the mineralogy of samples was interpreted based on the presence of diagnostic peaks. Results are reported as percentage of background sediment samples vs. event layers containing particular minerals (Figure 5.19). While all samples contained both kaolinite and montmorillonite (smectite), and about 25% of both the background and event sediments contained chlorite, there were some noticeable differences in the mineral content of the two sample categories.

Mica (biotite, muscovite, illite) was found in a higher percentage of the background sediment samples than in the event layers. As expected, fewer of the fine background sediments samples contained quartz than did the event layer samples. Due to the hardness and low solubility of quartz, it is more resistant to weathering than other minerals and therefore usually is larger than other mineral grains. Calcite was found in a small portion of the event layers, but was not seen in any background sediments. Feldspar content also was variable amongst the samples, and was present in about half as many background sediment samples as event layer samples (Figure 5.20).

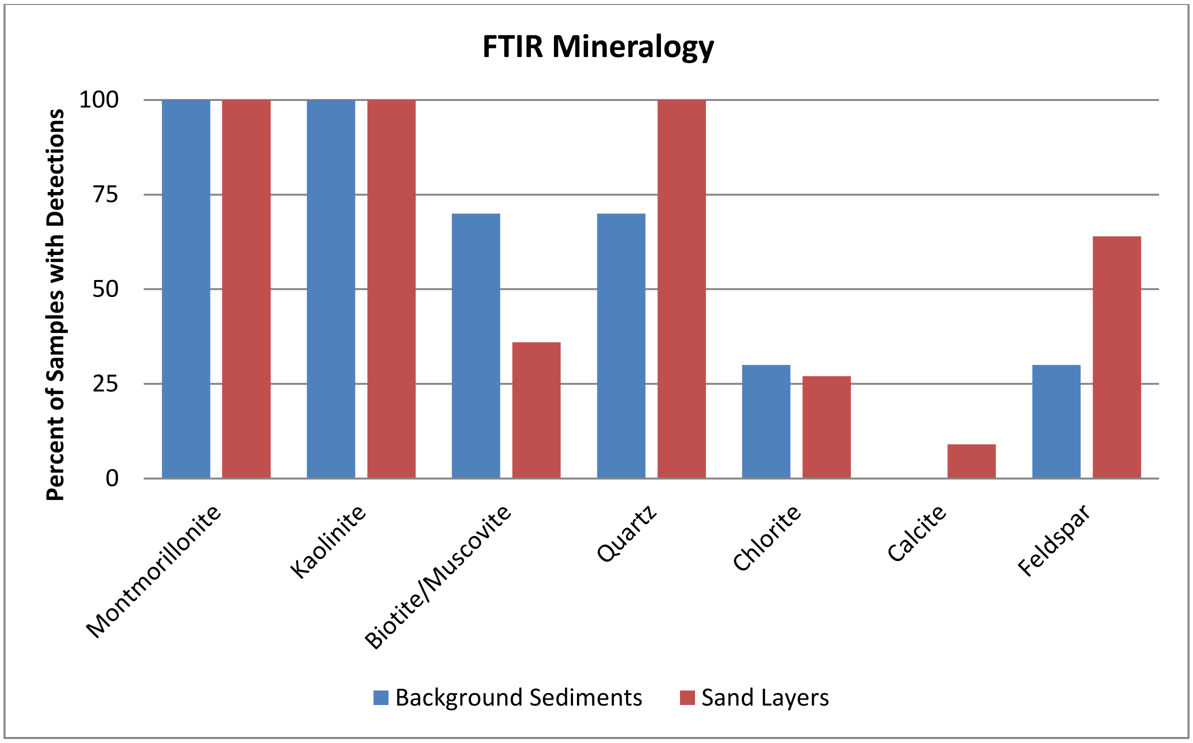

Figure 5.19 Percent of examined samples (11 background sediments and 10 event layers) in which identified minerals were detected. Note greater amount of quartz and feldspar in event layers compared to the background sediments.

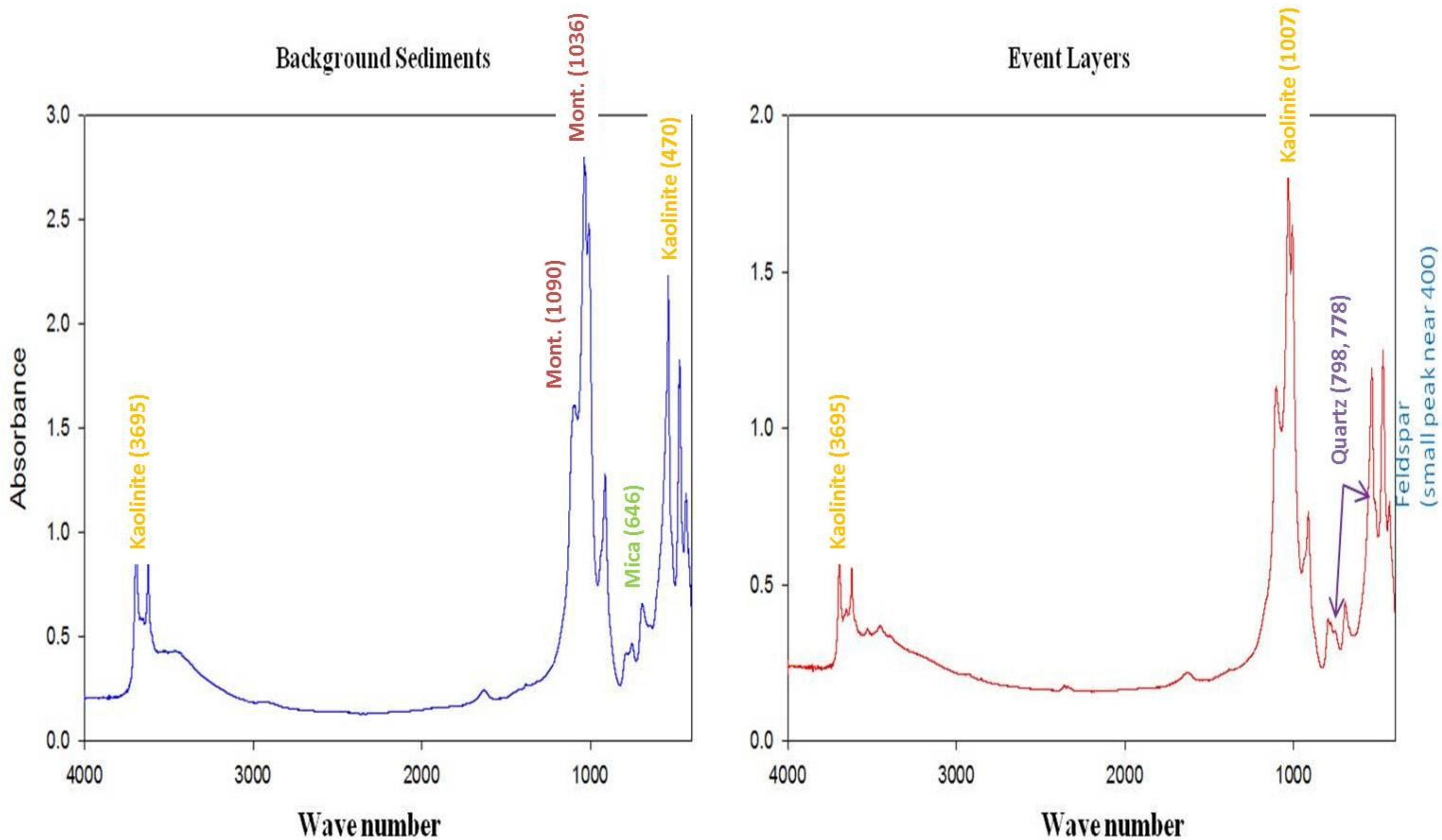

Figure 5.20 FTIR spectra with diagnostic peaks noted. Kaolinite, montmorillonite (mont.), and mica are prevalent in the background sediments (spectra from JDH-1-1 13cm). Kaolinite, quartz, and feldspar characterized the event layers (spectra from RC-3).

5.5 Sediment Dating Techniques

5.5.1 ^{210}Pb

^{210}Pb results are plotted against depth in the core (y-axis), and show that much variability exists in the calculated activities. ^{210}Pb interpretations are made assuming that the supply of ^{210}Pb was relatively constant through the millpond's history and therefore the profiles exhibit the classic profile (Campbell, 1996; Demaster et al., 1994; Jeter, 2000; Noller, 2000) of a surface-mixed layer (no change in activity), a zone of accumulation (used for rate estimations), and a zone of supported activity (vertical trend in the profile). The data from Mitchell Mill show this type of profile, but those from Yates Mill do not. The low total activity values indicate that the sediments at YM-1 are too old to have ^{210}Pb activity. A reasonable assumption is that due to natural erosion (by the stream) or dredging has removed more recent sediments. Whatever, the cause of the unexpected data trends, the results from the YM-1 profile were not used to estimate a sediment accumulation rate. However, since the MMP-2 profile appears to have some excess activity, an accumulation rate of 0.35 cm/yr. was calculated by dividing the decay rate by the slope of the excess ^{210}Pb activity. This value is nearly the same as the estimated accumulation rate based on the build and breach dates for the dam at Mitchell Mill, 0.32 cm/yr.

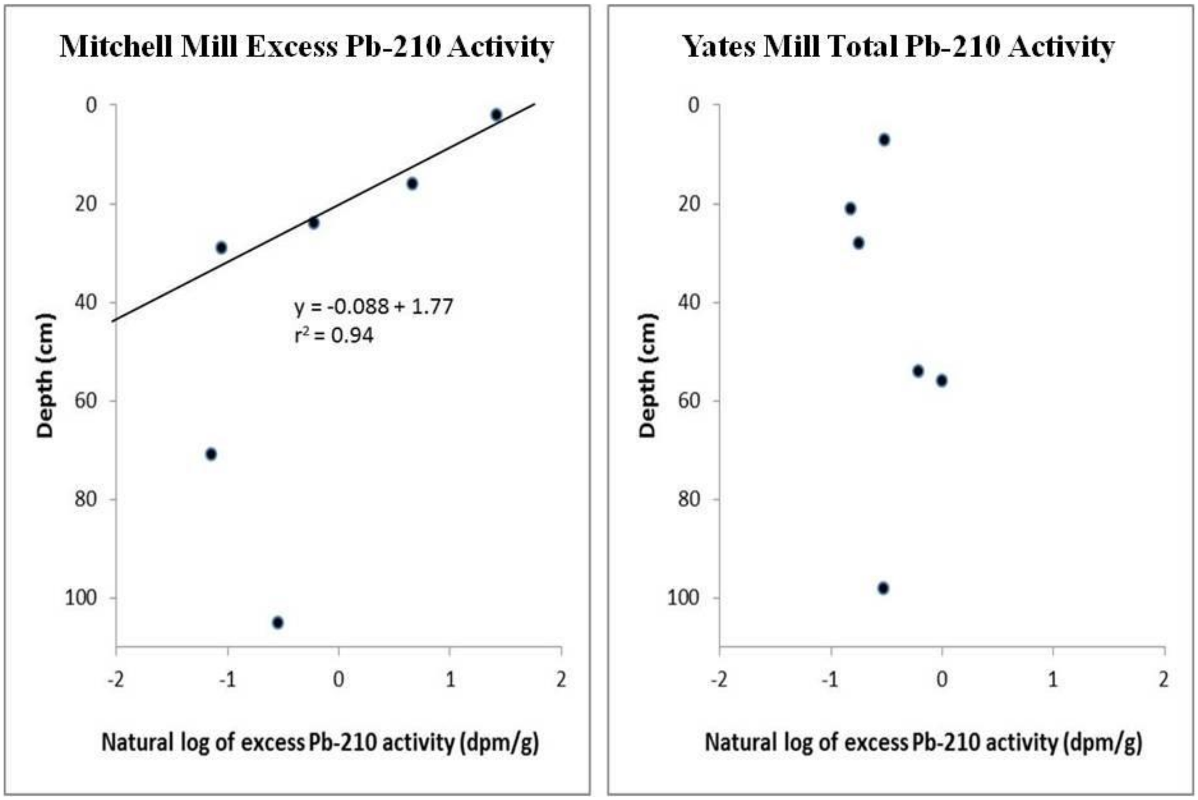

Figure 5.21 ^{210}Pb profiles from core MMP-2 (left) and YM-1 (right), with linear regression for Mitchell Mill. Activity in YM-1 was low throughout.

5.5.2 Dendrochronology

Of the 12 trees sampled, half of the cores had ring boundaries which were indistinguishable and could not accurately be measured. Also, the dates shown in Figure 5.22, are estimates, as false rings and missing age ranges (due to extreme droughts or other environmental factors) can account for inaccuracies in the data set. For the 6 trees from which chronologies could be established, the mean number of rings was 94, with the oldest having 102 rings (Figure 5.22). Since the trees were cored in 2010, the rings indicate that the dam breached and the trees began to grow on the exposed pond floor at Cook's Mill in 1916, six years later than is indicated by historical accounts. Given that it is reasonable to assume that it would take 5-6 years for trees to begin to grow and establish themselves on the millpond floor, the ring chronology seems to match very well with the historical records.

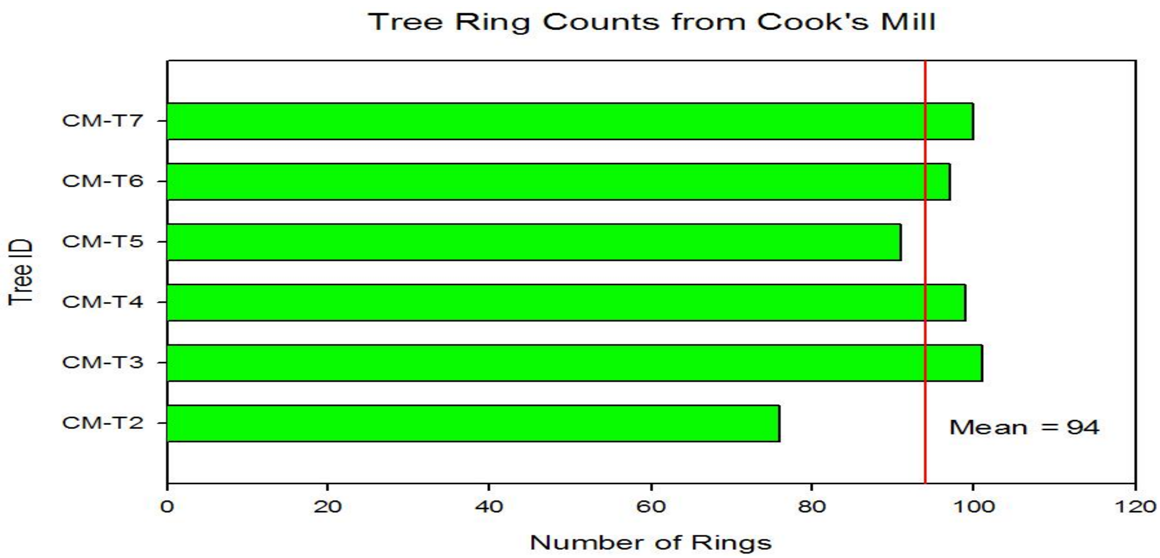

Figure 5.22 Dendrochronology results from Cook's Mill, showing ring counts from six trees which were located on the relic millpond floor. The trees are interpreted to have begun growing not long after the breach of the milldam in 1910.

5.6 Sedimentary Records at Each Millpond

<u>Cook's Mill</u>:

Accumulation rates at Betty's Mill and Cook's Mill were estimated using the thickness of the millpond deposits, therefore delineation of the age of sediments at the top and bottom of the deposits is key to producing accurate accumulation rate estimations. From historical deeds, dendrochronology, and landowner comments, it can be inferred with reasonable certainty the Cook's Millpond was built near 1798 and breached sometime around 1910, giving it a lifespan of 112 years. The entire thickness of the millpond sediments at Cook's Mill is 183 cm. In order to account for the sandy event layers in each profile, which are interpreted as being deposited "instantaneously" in time, their cumulative thickness (≈ 17 cm) was omitted from the millpond facies' total thickness. Therefore the average accumulation rate was approximately 1.48 cm/yr.

Betty's Mill:

No reliable historical data exists for Betty's Mill. It does not, however, appear on any of the historical maps, therefore, assuming that the 1871 map is accurate, it must have breached pre-1871 and as mentioned previously, due to the building techniques it is thought to predate 1810. Therefore, an accurate accumulation estimate is not ascertainable at this location, but a maximum rate is 1.86 cm/yr.

Yates Mill:

Yates Mill has the most complete and well documented history of all of the study sites. The mill was petitioned in 1756 and breached during hurricane Fran in 1996. Unfortunately, neither of the cores recovered in this study appear to preserve a complete record of this lengthy history. Near the dam, where currents tend to be stronger, YM-3 (Figure 3.3) was composed of mostly sandy sediments. Further upstream where the stream channel enters the pond, YM-1 sampled 87 cm of fine-grained pond sediment, however the low ^{210}Pb activity measured in these sediments suggests that the core material may be more than 100 years old and that this part of the pond was affected by natural erosion or dredging. Given the uncertainty of the age of the core material, it cannot be used for establishing a storm history.

JD Hayes' Mill:

Deed records indicate that JD Hayes' Mill (established initially as Park's Mill) was probably built near 1773. Due to its presence on the Bevers map of1871 and absence on the Shaffer map of 1887, the dam breach date was approximated as the midpoint of these records, or ca. 1879. Using this estimation, the mill was in existence for around 106 yrs. Cores JDH-1 and JDH-2 both sampled mostly coarse sediments (sands) that were likely deposited near the pond shoreline (Figure 5.14). The finer grained sediments near the tops of the cores likely record only a portion of the pond's history, and because of uncertainty in the amount of time these deposits represent, a calculation of accumulation rate or reconstruction of the pond's storm history has not been attempted.

Mitchell Mill:

Direct communication from the family that owned this property indicated that this mill was constructed in 1759, whereas court-documented petition records indicate the date was 1772 and this was used to approximate an accumulation rate. The dam is still in place, although the mill is long gone, so essentially there has been a structure continually trapping sediment at this site for 238 years. The estimated sediment accumulation rate based on the only complete core, MMP-2, (accounting for instantaneous deposition represented by the sand layers) 0.32 cm/yr., while the ^{210}Pb rate is 0.35 cm/yr. As a compromise between the results determined by these two different methods, a value of 0.34 cm/yr was used for further calculations.

Table 5.3 Sedimentary records preserved at each site.

Pond	Date of earliest deposition	Date of latest deposition	Time span (years)	Outcrops/Cores investigated	Thickness of fine millpond sediments (cm)	Estimated Accumulation Rate
Cook's	1798	1910	112	Outcrop	183	1.48 cm/yr
Betty's	Pre-1810	Pre-1871	>61?	Outcrop	205	1.86 cm/yr
JD Hayes	1773	1887	114	JDH-1 JDH-3	None 37	N/A N/A
Mitchell	1759	Present	252	MMP-1 MMP-2	None 111	N/A 0.34 cm/yr
Yates	1756	Present	245	YM-1 YM-3	90 35	N/A N/A

6.0 DISCUSSION

6.1 Evolution of Millponds and Their Fills

The data presented here shows that millponds are dynamic environments, where preservation of event layers is predominately controlled by the evolution of the pond through time. Several of the millponds experienced fluctuation in their shorelines, which was determined to be a limiting factor for storm record preservation. These fluctuations could record changes in pond levels due to natural causes (wetter/dryer years) as well as human activities (i.e., draw down of the ponds for milling). The fine-grained deposits that accumulate far from the ponds' shorelines are likely to be the most accurate recorders of storm events. The Mitchell Mill record from MMP-2 located nearer the center of the millpond illustrates how large storms can be recorded by sandy layers interstratified with fine grained material delivered to the pond during times of lower stream flow.

Millpond deposits by definition indicate that the millponds were filling in over time, which explains the upward coarsening trend in grain size observed in the background sediments in several of the deposits. The fill records and consequently storm records are inherently different depending on the sampling location within the pond. In areas where a delta was actively prograding into the pond and/or at the upstream end of the pond the sediments would be expected to record thicker, coarser event layers over time (although these trends might be obscured by variations in storm intensity and/or stream flow).

6.2 Recognition of Event Layers in Millpond Sediments

Relative to the finer grained background sediments, the millpond event layers are coarser, more quartz-rich, and contain larger woody fragments. Initially, it was hypothesized that these layers would consist primarily of sand sized material, however after performing grain size analysis this proved to not always be the case. Event layers are recognized as thin intervals in the bank exposures and cores that are coarse relative to the average particle size, but they range from sand to medium-fine silt. It is likely that the size of particles in these layers depends on the magnitude of stream flow during particular events as well as the characteristics of the pond environments in which they were deposited. The abundant wood debris within the event layers likely reflects the intense surface runoff that can occur during storms and that may wash terrestrial plant material into the streams and ponds from upstream reaches (Brown et al.; 2000 Noren et al., 2002).

6.3 Event Stratigraphy at the Mill Sites

Mitchell Mill:

MMP-1 is much shorter (33 cm) than MMP-2 (111 cm), and contains coarser and more closely spaced sand layers. The lack of thicker fine-grained deposits in MMP-1 likely reflects the recovery of the core from an area (Figure 5.5) where the bedrock came close to the surface (core barrel made contact with bedrock) and the main stream channel was near. It is likely that any fine grained deposits that accumulated at this site were commonly eroded away and therefore no reliable history is recorded in this core.

In contrast to MMP-1, MMP-2 appears to have been the most reliable sedimentary archive recovered in this study. This core is representative of an ideal archive: mostly fine-grained background sediments with interstratified coarse-grained layers, which can be interpreted as the result of intense precipitation events. In total there were eleven coarse layers recorded in MMP-2, which due to the reliability of the accumulation rate results can reasonably assigned approximate ages. Using the dam build date of 1759 and a constant accumulation rate of 0.32 cm/yr, event layers $M(2)_1$ and $M(2)_2$ record storms in the late 1700's and early 1800's storm respectively. An increase in storm activity is seen in the mid-1800's, where a cluster of storms are recorded. From this time forward, more definitive dates can be given using the US Geological Survey (USGS) stream data from the Neuse River (Figure 6.1).

The USGS has collected stream data from the Neuse River, near Clayton NC (in Johnston County, which is approximately 27 miles south of Mitchell Millpond,) since 1927. As shown in Figure 6.1, recent large named hurricanes, Fran and Dennis, identified in these stream data, are also recorded in the Mitchell Mill proxy data, along with possible unnamed category four hurricanes in 1946 and 1929. The data shown in Figure 6.1 indicate only the largest storms are recorded as discrete storm layers. Furthermore, as the Neuse River discharge record illustrates, there are plenty of high flows between the biggest storms, and therefore the "background sediments" incorporate sediments deposited under a range of flows. It is also apparent that the number of high discharge events varies over time (e.g. the 1950's to mid 1970's were stormier), so the assumption of constant sediment accumulation rates in millponds is likely to be inaccurate. This observation would explain why the 1946 and 1929 storms appear to be lower in the MMP-2 core than would be expected assuming a constant rate of sediment accumulation.

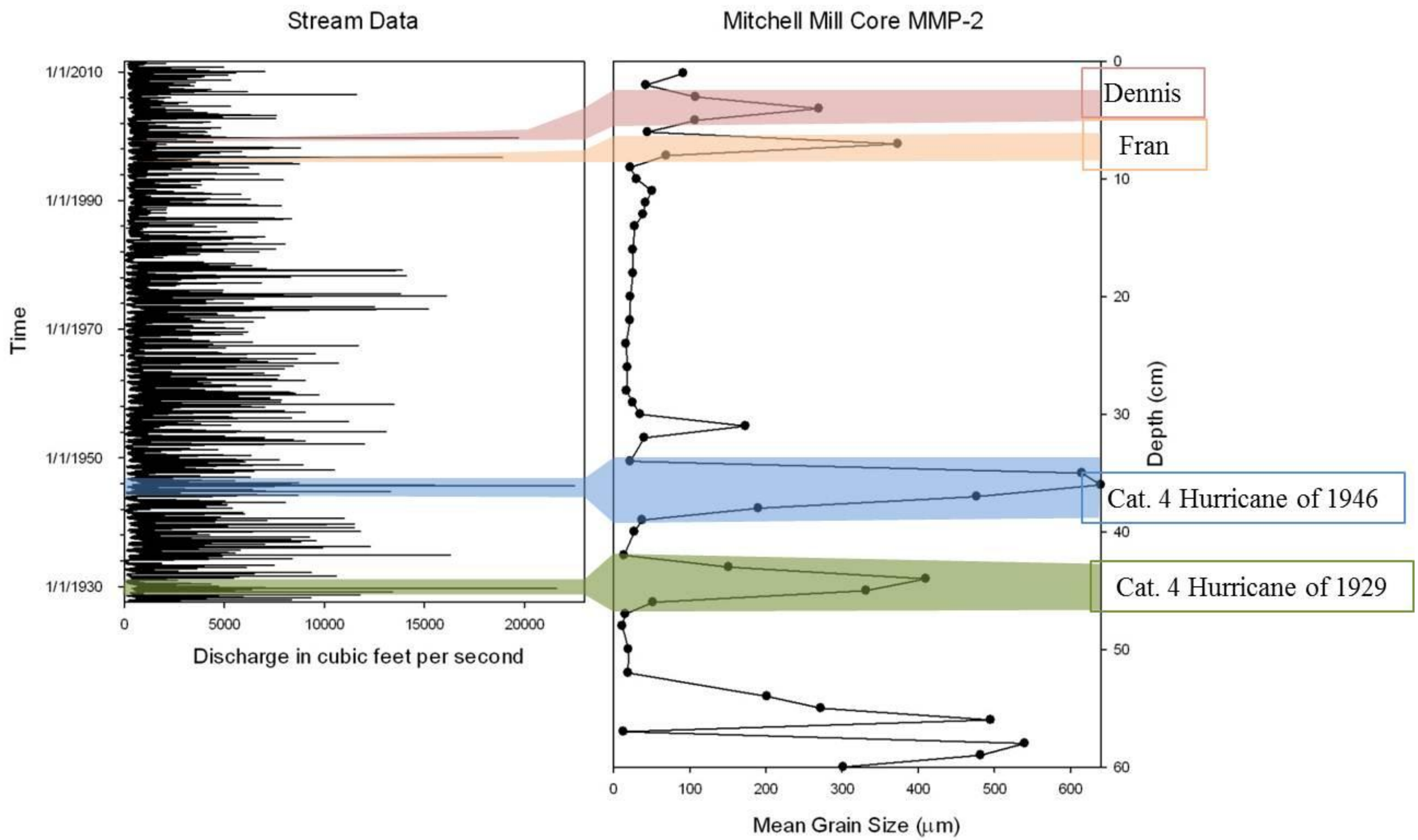

Figure 6.1 Comparison of USGS Stream Data from the Neuse River near Clayton, NC with the recorded grain size proxy history since 1880 (or 60 cm depth) based on accumulation rate estimates. Four major storms are identified: Dennis, Fran, and 2 unnamed storms of 1946 and 1929 (http://waterdata.usgs.gov/nwis/inventory?agency_cd=USGS&site_no=02087500).

Stratigraphic Profiles at Cook's Mill and Betty's Mill:

The close proximity and apparent age-overlap of the ponds at Betty's Mill and Cook's Mill suggests that they might record some of the same storm events, therefore they were compared to examine the proxy record from Umstead State Park. These stratigraphic profiles represent the most detailed records obtained in this study, as millimeter-scale layering can be visually identified in these two stream-bank exposures, whereas cores from the other sites were sampled at 1-cm resolution due to time and budget constraints. Only the thickest layers at Betty's Mill could be sampled and analyzed for particle size. The layers at Cook's Mill, however, were generally thicker, and therefore grain size analysis was performed on many of them as well as on interstratified background sediments.

It is apparent that the sediments behind Betty's Mill contain many more thin stormy layers than do those that accumulated behind Cook's Mill (Figure 6.2). This indicates that the catchment upstream of Betty's Mill was more sensitive to small storms and/or that the sample location of the pond was a better place to preserve the layers. The dam at Betty's Mill was two meters higher than at Cook's, yet the pond was much narrower (Figure 5.2). That difference indicates that the slopes at the pond margins were much steeper. Field observations found that the catchment had some steep hillsides with evidence for mass wasting just upstream of the Betty's Mill study site. This observation suggests that the stream feeding Betty's Mill, Reedy Creek, likely had a higher sediment load than Richland Creek which fed Cook's Millpond. Sediment was most likely mobilized from hillslopes even during moderate storms, and the thin sandy layers that resulted are separated by mud that may have accumulated between them. Also, Betty's Millpond sample site is near a tributary entrance into the stream which would have been a prograding delta into the center of the millpond (and therefore would have help to preserve this stratigraphy).

It is reasonable to assume based on their histories that these two sites had some overlap; however it is apparent from these interpretations (Figure 6.2) that their accumulation rates were very different. Upon comparison of the two sites as shown in Figure 6.2, it seems possible based on layer thickness and position within the stratigraphy that B_{20} correlates to C_5, and B_{23} correlates to layer C_9. This indicates that the deposits at Betty's Mill may be younger than previously thought (and was unrecorded on the Bevers map), since this time frame is more likely to correlate to the mid to late 1800's rather than to the early 1800's.

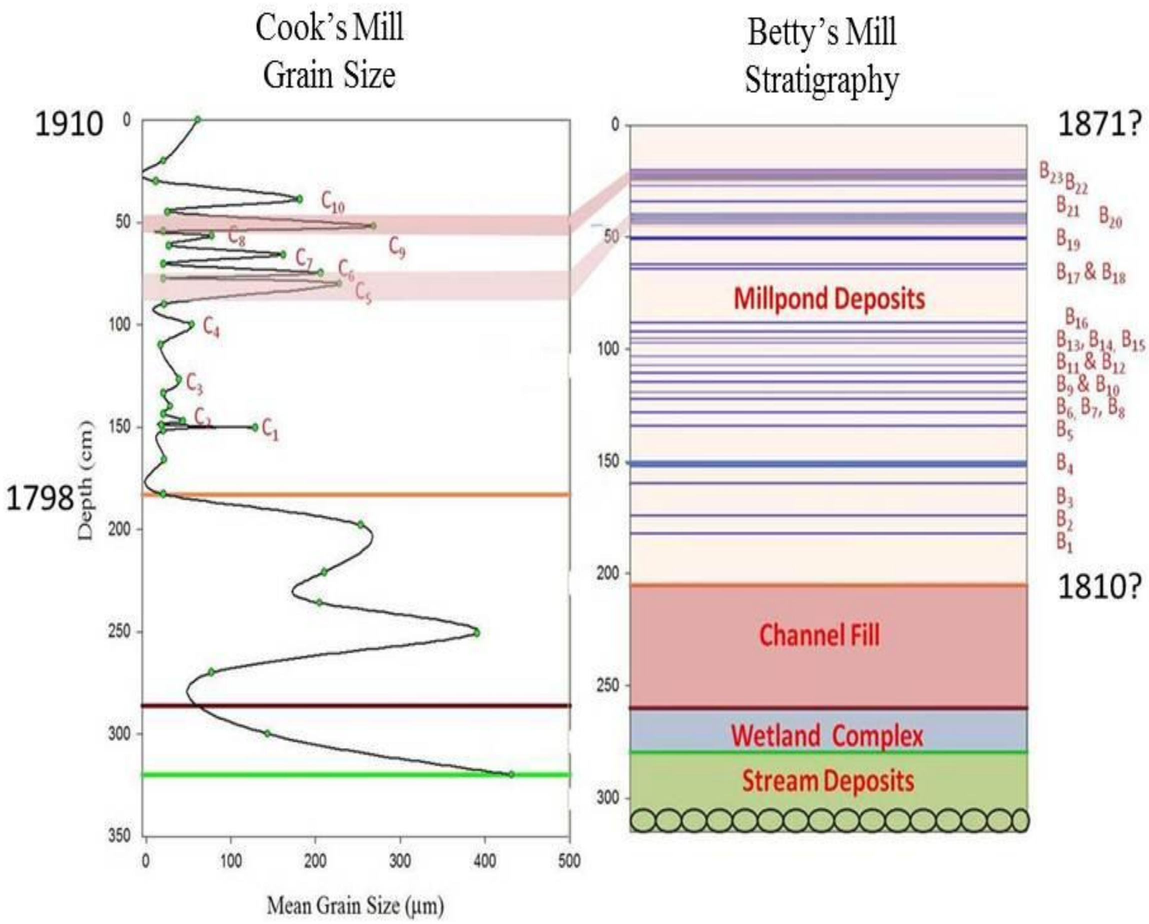

Figure 6.2 Position of Event Layers identified in the grain size data from Cook's Mill and from the stratigraphic profile at Betty's Mill. Estimated build dates (bottom) and breach dates (top) of dams at each site are noted. Event correlations based on position and thickness of event layers in stratigraphic profiles. Red bars indicate events that are correlative in each profile.

Yates Mill:

While YM-1 is characterized by the typical fine millpond sediments with interstratified sandy storm layers, due to the ^{210}Pb data, the reliability of the data for accurate storm estimates is questionable. However, there is a historical record of a large storm which was severe enough to put the mill out of operation dated "pre-1820" (Yates Mill History, 2010). This event may have caused a breach in the dam and may be the origin of the coarse deposit at the bottom of the core. Without a definitive correlation with this event at the bottom of the core, the preserved record is unreliable for storm evaluations at this point.

In the upper portion of core YM-3 there appears to be at least one definitive storm event recorded. However, coarser layers in the lower portion of core YM-3 may record longer–term fluctuations in the position of the pond shoreline, rather than storm events (Figure 5.13). As shown in Figure 5.3, YM-3 is close to the existing pond shoreline, which based on the estimated relic surface has remained relatively close to the modern day position throughout the ponds' history. There is no existing historical record of pond water levels; however it can be inferred from core YM-3 that the pond has experienced multiple shoreline regressions/transgressions in response to dry/wet periods and/or variable water use during mill operations.

JD Hayes' Mill:

The upper 36 cm from core JDH-2 are the only fine-grained millpond sediments recovered from the JD Hayes site. Within these deposits are three possible mid-late 1800's event layers. Below 36 cm, JDH-2 exhibits characteristics similar to YM-3, which is more representative of fluctuations in the shoreline. The lack of fine-grained sediments in the JDH-1 core is likely due to sediment erosion after the breach of the millpond in 1879 (Note the proximity of JDH-1 to the milldam in Figure 5.4).

6.4 Possible Storms Recorded in the Archive

ArcGIS proved to be a very useful tool in this study for identifying storms (tropical cyclones) that passed close to the study sites. Initially, data were retrieved for storms which passed within 50 and 15 miles of Wake County, however due to the large number of results and relative uncertainty in the data (due to its reliance on historical accounts) it was apparent these results would not be useful for attributing storm layers in the millpond sediments to particular events. In addition, when larger radii were used, certain time intervals would have multiple events occurring at nearly the same times, which further complicated the correlation of specific storms to the event layers. It is understood that using a smaller distance may omit some severe storms which could have had a large impact on the study area. Also, due to the reliance on tropical cyclones as "severe recorded storms," intense single cell summer convection thunderstorms which are more stochastic and frequent at the scale of these small drainage basins are unaccounted for in these results. Twenty-four storms which passed within a radius of two miles of the study sites in Wake County were identified (Figure 6.1) in the historical record (NC State Climate Office, 2010). Prior to

1851, only general descriptions of storms are available, therefore storms (tropical cyclones) which were mentioned to have come inland near Wake County were the only storms identified as having a potential impact on the study sites (Table 6.2). The data from this time period were taken from Hudgins (1966) who compiled a detailed listing of all the known written records of tropical cyclones since 1586.

The layers identified in the millpond deposits are tentatively attributed to storms in historical records as follows: 1) a late 1700's storm recorded by B_4 and $M(2)_1$, $M(2)_2$ may correspond to a severe storm known to have come inland and caused major damage as far west as Winston Salem in 1783, 2) A mid to late 1800's storm recorded at Cook's and Betty's Mill by layers C_9 and B_{23}, which possibly could correlate to the 1846 storm which was reported to have moved inland over North Carolina,. 3) A cluster of mid 1800's storms recorded by layers at Cooks, JD Hayes, Mitchell Mill, and possibly also Betty's Mill, which are most likely correlative to the cluster of recorded storms during this same time interval (see Table 6.1); and 4) hurricanes of 1910, 1929, 1946, Fran, and Dennis, recorded in MMP-2.

Table 6.1 Storm Tracks recorded within 2 miles of Wake County since 1851.

Year	Storm Name	Category
1877	Not Named	Hurricane: Category 3 (H3)
1886	Not Named	Tropical Depression (TD)
1888	Not Named	Tropical Storm (TS)
1889	Not Named	Hurricane: Category 2 (H2)
1893	Not Named	Hurricane: Category 3 (H3)
1899	Not Named	Hurricane: Category 2 (H2)
1902	Not Named	Tropical Storm (TS)
1904	Not Named	Hurricane: Category 1 (H1)
1929	Not Named	Hurricane: Category 4 (H4)
1940	Not Named	Tropical Depression (TD)
1946	Not Named	Hurricane: Category 4 (H4)
1954	Hazel	Hurricane: Category 4 (H4)
1955	Diane	Hurricane: Category 3 (H3)
1968	Celeste	Tropical Storm (TS)
1970	Alma	Hurricane: Category 1 (H1)
1971	Unamed	Tropical Depression (TD)
1971	Heidi	Tropical Storm (TS)
1976	Unamed	Tropical Storm (TS)
1987	Unamed	Tropical Depression (TD)
1996	Fran	Hurricane: Category 3 (H3)
1999	Dennis	Hurricane: Category 2 (H2)
2000	Gordon	Hurricane: Category 1 (H1)
2004	Gaston	Hurricane: Category 1 (H1)

Table 6.2 Recorded Storm Events from Hudgins, 1996

Storm Date	Description
Oct. 7-8, 1783	Damage reported as far west as Winston-Salem
Sept. 10, 1811	Severe in inland SC, probably tracked north causing damage in NC
Sept. 27-28, 1822	Violent winds and torrential rains affected Raleigh.
Sept. 4, 1834	Heavy rains produced flooding on the Neuse River and wind blew down trees in central NC.
August 18-20, 1837	All bridges between Wilmington and Goldsboro were destroyed.
Oct. 12, 1846	Struck the Florida Keys and moved inland over central NC.

Storms possibly tracking near Raleigh, NC, recorded before 1851 ca. compiled by Hudgins, 1966.

7.0 CONCLUSIONS AND SUMMARY

A potential new proxy record for high intensity storm events occurring after colonization of the Piedmont region of North Carolina was presented, using millponds in Wake County as a pilot project. The results of this study indicate that millponds are dynamic environments. Their sizes and the position of their shorelines will vary over time both due to climate (wet years, droughts) and also because of human activities. The fine-grained deposits that accumulate far from the ponds' shorelines are likely to be the most faithful recorders of storm events. The Mitchell Mill record illustrates how large storms can be recorded by sandy layers interstratified with fine- grained material delivered to the pond during times of lower stream flow. The differences between the sedimentary records of the Cook's and Betty's millponds illustrate how one pond can be more sensitive to small events than another. Also, with time, the ponds fill in, and as a delta at the upstream end progrades into the pond, the background sediments as well as storm deposits tend to get coarser and thicker. The upstream pond reaches will transition from states of deposition, to zones of sediment transport, bypass, and potentially erosion as the pond fills in.

Grain size analysis revealed that generally fine-grained millpond sediments are punctuated by thin, sand layers interpreted to record high intensity storm events. These layers are commonly rich in plant debris and they contain a greater percentage of quartz and feldspar grains than do finer grained background sediments. Through a variety of dating approaches, some of these layers can be attributed to known historical events and some can be correlated with some confidence from one pond deposit to another, but in other cases it is not possible to attribute them to specific storms. Prevailing ideas about climate and flood recurrence intervals are based in part on historical accounts which may need to be modified in the future. Intense storms are predicted to increase in the future (Storen et al., 2010), but as shown in this record storm variability since colonization has been the norm. The potential utility of this proxy is apparent, but clearly more research is needed before that potential can be realized.

The goal of this study was to evaluate the hypothesis that a storm history for the Piedmont region of North Carolina can be extended back beyond the length of reliable written records and improved using millpond sediments. Initial findings indicate that there is a high probability that storm events which were previously unrecorded may be discovered by evaluating the grain size trends within these sedimentary archives. Further data are needed to establish the extent and particularly the timing of storms indicated by the results of this study.

8.0 REFERENCES

Basinwide Assessment Report for the Neuse River Basin. Ed. North Carolina. Division of Environmental Management. Water Quality Section. Raleigh, N.C.: North Carolina Department of Environment, Health, and Natural Resources, 2001. Book; 254 p..

*State Climate Office of North Carolina.*Web. <http://www.nc-climate.ncsu.edu/>.

"US Census, 1860."Web. <http://www.census.gov/prod/www/abs/decennial/1860.html>.

Water Resources Data. North Carolina [Electronic Resource]. Ed. Geological Survey (U.S.). Raleigh, N.C.: U.S. Dept. of the Interior, U.S. Geological Survey : Prepared in cooperation with the North Carolina Department of Environment and Natural Resources, and with other State, municipal <http://www2.lib.ncsu.edu.www.lib.ncsu.edu:2048/catalog/record/DWSb4907025>.

"Aerial photo collection: Wake County, 1959." 2011, Feb. 23, USDA Farm Service Agency. <www.fsa.usda.gov>.

Almquist, Katherine. "The Weathering of Volcanic Ash and Resultant Clay Minerals in a Terrestrial and Marine Environment: North Island, New Zealand." Master of Science North Carolina State University, 2010. Print.

Applequist, MB. "A Simple Pith Locator for use with Off-Center Increment Cores." *Journal of Forestry* 56.141 (1958): 141.

Benedetti, M. M., et al. "Mineralogical Indicators of Alluvial Sediment Sources in the Cape Fear River Basin, North Carolina." *Physical Geography* 27.3 (2006): 258-81.

Bevers, Fendol. Map of Wake County Nichols & Gorman, 1871. 1:126,720, Wake County, N.C. UNC Libraries (Jan. 2010).
http://dc.lib.unc.edu/cdm4/item_viewer.php?CISOROOT=/ncmaps&CISOPTR=241.

Brown, S. L., et al. "10 000 Yr Record of Extreme Hydrologic Events." *Geology* 28.4 (2000): 335.

Campbell, C. "Late Holocene Lake Sedimentology and Climate Change in Southern Alberta, Canada." *Quaternary Research* 49.1 (1998): 96-101.

Campbell, I. D. "Power Function for Interpolating Dates in Recent Sediment." *Journal of Paleolimnology* 15.1 (1996): 107-10.

Certini, G., et al. "Mineral Weathering in Trachydacitic-Derived Soils and Saprolites Involving Formation of Embryonic Halloysite and Gibbsite at Mt. Amiata, Central Italy." *Geoderma* 133.3-4 (2006): 173-90.

Clark, S. L., and S. W. Hallgren. "Age Estimation of Quercus Marilandica and Quercus Stellata: Applications for Interpreting Stand Dynamics." *Canadian Journal of Forest Research* 34.6 (2004): 1353-8.

Cranmer, E. "Stratigraphic Reconstruction of Holocene Paleogeography and Paleoclimate, Little Falls, MD." (2009)

Czymzik, M., et al. "A 450 Year Record of Spring-Summer Flood Layers in Annually Laminated Sediments from Lake Ammersee (Southern Germany)." *Water Resources Research* 46.11 (2010): W11528.

Daniels, Raymond Bryant, 1925-. *Soil Systems in North Carolina*. Ed. North Carolina State University. Soil Science Dept. Raleigh, N.C.: North Carolina State University, Soil Science Department, 1999.

Dearing, JA. "Lake Sediment Records of Erosional Processes." *Hydrobiologia* 214.1 (1991): 99-106.

DeMaster, D. J., et al. "Biological Mixing Intensity and Rates of Organic Carbon Accumulation in North Carolina Slope Sediments." *Deep Sea Research Part II: Topical Studies in Oceanography* 41.4-6 (1994): 735-53.

Easterling, D. R., et al. "Climate Extremes: Observations, Modeling, and Impacts." *Science* 289.5487 (2000): 2068.

Eden, D. N., and M. J. Page. "Palaeoclimatic Implications of a Storm Erosion Record from Late Holocene Lake Sediments, North Island, New Zealand." *Palaeogeography, Palaeoclimatology, Palaeoecology* 139.1-2 (1998): 37-58.

Enfield, D. B., A. M. Mestas-Nunez, and P. J. Trimble. "The Atlantic Multidecadal Oscillation and its Relationship to Rainfall and River Flows in the Continental US." *Geophys.Res.Lett* 28 (2001): 2077–2080.

Farmer, VC, and JD Russell. "Infrared Absorption Spectrometry in Clay Studies." *Clays and Clay Minerals* 15.1 (1967): 121-14.

Flett, Robert. "Understanding the Pb-210 Method." Jan 7, 2009 2009.Web. <http://www.flettresearch.ca/Webdoc4.htm>.

Flynn, WW. "The Determination of Low Levels of Polonium-210 in Environmental Materials." *Analytica Chimica Acta* 43 (1968): 221-7.

Grissino-Mayer, H. D. "A Manual and Tutorial for the Proper use of an Increment Borer." *Tree-Ring Research* 59.2 (2003): 63-79.

Hart, BS, and BF Long. "Storm Deposits from the Quaternary Outardes Delta, Quebec, Canada." *Sedimentary Geology* 67.1-2 (1990): 1-5.

Haven, Walter T., 1968-. "Reservoir Sedimentation in the North Carolina Piedmont." North Carolina State University -- Theses -- Marine, Earth and Atmospheric Sciences. 2000.

Heikkinen, O. "Using Dendrochronology for the Dating of Land Surfaces." *Dating in exposed and surface contexts/Beck, C.(ed.).–University of New Mexico Press, Albuquerque* (1994): 213–235.

Hiskin, Larry A. *The Atomic Nucleus and Chemistry*. Canada: D. C. Heath and Company, 1972.

Hudgins, J. E. "Tropical Cyclones Affecting North Carolina since 1586-an Historical Perspective." *Forest* (2000). http://www.erh.noaa.gov/er/hq/ssd/erps/tm/tm100.pdf (Jan. 2010).

Jackson, CR, et al. "A Southeastern Piedmont Watershed Sediment Budget: Evidence for a Multi-Millennial Agricultural Legacy." *Journal of Soil and Water Conservation* 60.6 (2005): 298.

Jeter, H. W. "Determining the Ages of Recent Sediments using Measurements of Trace Radioactivity." *Terra et Aqua* 78 (2000): 21-8.

Kautzman, Robert Ronald, 1945-. *Temporal Relations between Urbanization and Sedimentation: Lake Boone, Raleigh, North Carolina*. Raleigh, N.C., 1972, 1972.

Kotarba, A., E. Łokas, and P. Wachniew. "210Pb Dating of Young Holocene Sediments in High-Mountains Lakes of the Tatra Mountains." *Geochronometria* 21 (2002): 73-7.

Kuehl, S. A., D. J. DeMaster, and C. A. Nittrouer. "Nature of Sediment Accumulation on the Amazon Continental Shelf." *Continental Shelf Research* 6.1-2 (1986): 209-25.

Lewis, Robert. "The Lasting Impacts of Post-Colonial Agriculture and Water-Powered Milldams on Current Water Quality, Wake County, Raleigh, North Carolina." Master of Science North Carolina State University, 2011.

Leigh, D. S. "Late Quaternary Climates and River Channels of the Atlantic Coastal Plain, Southeastern USA." *Geomorphology* 101.1-2 (2008): 90-108.

Madejova, J., and P. Komadel. "Baseline Studies of the Clay Minerals Society Source Clays: Infrared Methods." *Clays and Clay Minerals* 49.5 (2001): 410.

Mangili, C., et al. "Microfacies of Detrital Event Layers Deposited in Quaternary Varved Lake Sediments of the Piànico-Sèllere Basin (Northern Italy)." *Sedimentology* 52.5 (2005): 927-43.

Marel, H. W., and H. Beutelspacher. *Atlas of Infrared Spectroscopy of Clay Minerals and their Admixtures.* Elsevier Publishing Company., 1976.

Michelsen, Erik. "The South River, Legacy Sediments, and the Future of the Resource." *Water Resources Impact* 11.5 (2009): 3-4.

Milly, PCD, et al. "Increasing Risk of Great Floods in a Changing Climate." *Nature* 415.6871 (2002): 514-7.

Munsell Color (Firm). *Munsell Soil Color Charts*. Baltimore, Md.: Munsell, 1954. Web.

Nichols, Gary. "Sedimentology and stratigraphy." 2009.

Nittrouer, CA, et al. "The use of Pb-210 Geochronology as a Sedimentological Tool: Application to the Washington Continental Shelf." *Marine Geology* 31.3-4 (1979): 297-316.

Noller, J. S. "Lead-210 Geochronology." *Quaternary geochronology: methods and applications* (2000): 115–120.

Noren, A. J., et al. "Millennial-Scale Storminess Variability in the Northeastern United States during the Holocene Epoch." *Nature* 419.6909 (2002): 821-4.

North Carolina State Archives. *Wake County Land Records: Deeds*., 1774-1940.

North Carolina Wildlife Resources Commission. 2011. <http://www.ncwildlife.org/plan/documents/NeuseRiverBasin/NRB-Full.pdf>. "N.C. River Basin Map."

Nyberg, J., et al. "Low Atlantic Hurricane Activity in the 1970s and 1980s Compared to the Past 270 Years." *Nature* 447.7145 (2007): 698-701.

O'Driscoll, MA, Riggs, SR; Ames, DV; Brinson, MM; Corbett, DR; Mallinson, DJ. "Geomorphic, Ecologic, and Hydrologic Dynamics of Merchants Millpond, North Carolina". "International Conference on Hydrology and Management of Forested Wetlands." Vol. 8, 12-18.

Ohashi, F., et al. "Synthetic Allophane from High-Concentration Solutions: Nanoengineering of the Porous Solid." *Clay Minerals* 37.3 (2002): 451.

Osleger, D. A., et al. "Lacustrine Turbidites as Indicators of Holocene Storminess and Climate: Lake Tahoe, California and Nevada." *Journal of Paleolimnology* 42.1 (2009): 103-22.

Phillips, J. D. "Delivery of upper-basin Sediment to the Lower Neuse River, North Carolina, USA." *Earth Surface Processes and Landforms* 17.7 (1992): 699-709.

Pironon, J., et al. "Characterization of Smectite and Illite by FTIR Spectroscopy of Interlayer NH4 Cations." *Clay Minerals* 38.2 (2003): 201.

Post, J. L., and L. Borer. "Physical Properties of Selected Illites, Beidellites and Mixed-Layer Illite-Beidellites from Southwestern Idaho, and their Infrared Spectra." *Applied Clay Science* 22.3 (2002): 77-91.

Riggsbee, J. A., et al. "Suspended Sediment, Dissolved Organic Carbon, and Dissolved Nitrogen Export during the Dam Removal Process." *Water Resources Research* 43.9 (2007): W09414.

Russell, J. D. "Infrared Spectroscopy of Inorganic Compounds." *Laboratory Methods in Infrared Spectroscopy*.

Russell, M., RL Parfitt, and GGC Claridge. "Estimation of the Amounts of Allophane and Other Materials in the Clay Fraction of an Egmont Loam Profile and Other Volcanic Ash Soils, New Zealand." *Australian Journal of Soil Research* 19.3 (1981): 185-95.

Schenk, E. R., and C. R. Hupp. "Legacy Effects of Colonial Millponds on Floodplain Sedimentation, Bank Erosion, and Channel Morphology, Mid-Atlantic, USA." *JAWRA Journal of the American Water Resources Association* 45.3 (2009): 597-606.

Schumm, S. A., and Colorado State University Fort Collins Dept. Of Earth Resources. *Evolution and Response of the Fluvial System, Sedimentologic Implications*. SEPM, 1981.

Seilacher, A., and T. Aigner. "Storm Deposition at the Bed, Facies, and Basin Scale: The Geologic Perspective." *Cycles and events in stratigraphy* (1991): 249-67.

Selley, R. C. *Applied Sedimentology*. Academic press, 2000.

Shaffer's Map of Wake County, N.C., 1887. Scale: 1:33,581. Wake County, NC. UNC Libraries (Jan. 2010). http://dc.lib.unc.edu/cdm4/item_viewer.php?CISOROOT=/ncmaps&CISOPTR=255&CISOBOX=1&REC=6.

Siegenthaler, C., and M. Sturm. "The Frequence of the Deposits of the Reuss Floods: The Sedimentation Story in the Uri Lake since the Middle Age." *Communication - National Hydrological and Geological* (1991).

Speer, James H., 1971-. *Fundamentals of Tree-Ring Research*. Tucson: University of Arizona Press, 2010.

Stahle, D. W., and M. K. Cleaveland. "Reconstruction and Analysis of Spring Rainfall Over the Southeastern US for the Past 1000 Years." *Bulletin of the American Meteorological Society;(United States)* 73.12 (1992).

Stoi, C., and J. Grtjnert. "Floodplain Sediments of some Streams in the Taunus and Westerwald Mts., Western Germany, as Evidence of Historical Land use." (2008).

Støren, E. N., et al. "Identifying the Sedimentary Imprint of High-Frequency Holocene River Floods in Lake Sediments: Development and Application of a New Method." *Quaternary Science Reviews* (2010).

Sturm, M., and A. Matter. "Turbidites and Varves in Lake Brienz (Switzerland): Deposition of Clastic Detritus by Density Currents." *Modern and Ancient Lake Sediments* (1978).

United States, Census Office. *A Compendium of the Ninth Census : (June 1, 1870,) : Compiled Pursuant to a Concurrent Resolution of Congress, and Under the Direction of the Secretary of the Interior*. Ed. Francis Amasa Walker. Washington, D.C. U.S. Government Printing Office, 1872, 1872.

Volnout, Vince. "Geo-Core sediment coring system."Web. 04/07/2011 <http://www.geo-core.com/>.

Wake County. "Yates Mill History." <http://www.wakegov.com/parks/yatesmill/history/default.htm>.

Walter, R., D. Merritts, and M. Rahnis. "Estimating Volume, Nutrient Content, and Rates of Stream Bank Erosion of Legacy Sediment in the Piedmont and Valley and Ridge Physiographic Provinces, Southeastern and Central Pennsylvania." *Report to the Pennsylvania Department of Environmental Protection, Lancaster, Pennsylvania* (2007).

Walter, R. C., and D. J. Merritts. "Natural Streams and the Legacy of Water-Powered Mills." *Science* 319.5861 (2008): 299.

Wiles, G. C., P. E. Calkin, and G. C. Jacoby. "Tree-Ring Analysis and Quaternary Geology: Principles and Recent Applications." *Geomorphology* 16.3 (1996): 259-72.

Wilson, M. J. *Clay Mineralogy: Spectroscopic and Chemical Determinative Methods*. Chapman & Hall London, 1994.

Wilson, William F. *Region J Geology : A Guide for North Carolina Mineral Resource Development and Land use Planning*. Ed. North Carolina. Geological Survey Section.

Raleigh, N.C. (P.O. Box 27687, Raleigh 27611): North Carolina Geological Survey Section, North Carolina Dept. of Natural Resources & Community Development, 1981.

Xue, Z., et al. "Late Holocene Evolution of the Mekong Subaqueous Delta, Southern Vietnam." *Marine Geology* 269.1-2 (2010): 46-60.

APPENDICES

9.1 Mean Grain Size Data, Cook's Mill

Cook's Mill		
Sample ID	Depth (cm)	Grain Size (μm)
RC-1	0	60.96
RC-2 LE	30	11.97
RC-3 SL	39	181.42
RC-4 LE	45	25.11
RC-5 SL	52	268.86
RC-6 SL	56.8	77.47
RC-7 LE	61.6	26.98
RC-8 SL	66.1	162.03
RC-9 SL	75	206.18
RC-10 SL	80	228.24
RC-11 LE	90	21.30
RC-12 SL	100	54.08
RC-13 LE	110	17.36
RC-14 SL	127	38.9526
RC-15 SL	140	28.5774
RC-16 SL	147.5	43.4531
RC-17 LE	149	18.3705
RC-18 LE	166	21.3553

9.2 Mean Grain Size Data, Betty's Mill

Betty's Mill		
Sample ID	Depth (cm)	Grain Size (μm)
BM-1 SL	22	420.90
BM-2 LE	30	125.78
BM-3 SL	41.5	586.79
BM-4 SL	159.5	698.55

9.3 Mean Grain Size Data, Yates' Mill

Yate's Mill Core YM-1		
Sample ID	Depth (cm)	Grain Size (µm)
YM1-1 23cm	1	53.55
YM1-1 21cm	3	35.59
YM1-1 19cm	5	27.41
YM1-1 17cm	7	24.17
YM1-1 15cm	9	32.38
YM1-1 14cm	10	43.67
YM1-1 13cm	11	44.83
YM1-1 12cm	12	40.47
YM1-1 11cm	13	27.59
YM1-1 9cm	15	30.45
YM1-1 7cm	17	34.58
YM1-1 6cm	18	39.02
YM1-1 5cm	19	58.08
YM1-1 4cm	20	57.27
YM1-1 3cm	21	30.32
YM1-1 1cm	23	35.77
YM1-2 73cm	26	26.62
YM 1-2 71cm	28	26.81
YM1-2 69cm	30	29.40
YM1-2 67cm	32	28.83
YM1-2 65cm	34	28.64
YM1-2 63cm	36	25.75
YM1-2 62cm	37	54.14
YM1-2 61cm	38	29.59
YM1-2 60cm	39	31.62
YM1-2 59cm	40	28.95
YM1-2 57cm	42	17.93
YM1-2 56cm	43	25.46
YM1-2 55cm	44	21.32
YM1-2 54cm	45	23.03
YM1-2 53cm	46	18.35
YM1-2 51cm	48	20.53
YM1-2 49cm	50	26.42

Core YM-1 Continued...		
Sample ID	Depth (cm)	Grain Size (µm)
YM1-2 47cm	52	22.23
YM1-2 46cm	53	24.59
YM1-2 45cm	54	25.13
YM1-2 44cm	55	24.62
YM1-2 43cm	56	19.97
YM1-2 41cm	58	18.17
YM1-2 39cm	60	19.03
YM1-2 37cm	62	18.93
YM1-2 35cm	64	15.09
YM1-2 33cm	66	19.77
YM1-2 31cm	68	19.36
YM1-2 29cm	70	21.56
YM1-2 27cm	72	21.51
YM1-2 25cm	74	24.94
YM1-2 23cm	76	24.73
YM1-2 22cm	77	30.48
YM1-2 21cm	78	26.20
YM1-2 20cm	79	22.56
YM1-2 19cm	80	19.71
YM1-2 17cm	82	19.68
YM1-2 16cm	83	23.18
YM1-2 15cm	84	23.28
YM1-2 14cm	85	25.05
YM1-2 13cm	86	21.18
YM1-2 11cm	88	17.59
YM1-2 9cm	90	17.50
YM1-2 7cm	92	220.47
YM1-2 5cm	94	860.53
YM1-2 3cm	96	37.59
YM1-2 1cm	98	19.81

Core YM-3		
Sample ID	Depth (cm)	Grain Size (µm)
YM-3-1 83cm	1	29.47
YM-3-1 82cm	2	32.53
YM-3-1 81cm	3	29.21
YM-3-1 80cm	4	29.84
YM-3-1 79cm	5	26.62
YM-3-1 77cm	7	20.40
YM-3-1 75cm	9	9.70
YM-3-1 73cm	11	12.90
YM-3-1 71cm	13	11.64
YM-3-1 69cm	15	7.30
YM-3-1 67cm	17	8.35
YM-3-1 66cm	18	13.35
YM-3-1 65cm	19	18.75
YM-3-1 63cm	21	16.46
YM-3-1 61cm	23	8.25
YM-3-1 59cm	25	6.49
YM-3-1 57cm	27	6.29
YM-3-1 55cm	29	9.32
YM-3-1 53cm	31	10.47
YM-3-1 51cm	33	9.97
YM-3-1 49cm	35	13.42
YM-3-1 48cm	36	338.08
YM-3-1 47cm	37	356.45
YM-3-1 46cm	38	608.79
YM-3-1 45cm	39	341.61
YM-3-1 44cm	40	508.59
YM-3-1 43cm	41	344.53
YM-3-1 42cm	42	184.11
YM-3-1 41cm	43	353.66
YM-3-1 40cm	44	346.63
YM-3-1 39cm	45	7.64
YM-3-1 37cm	47	7.20
YM-3-1 35cm	49	445.78
YM-3-1 34cm	50	23.37
YM-3-1 33cm	51	629.47
YM-3-1 32cm	52	648.84

Core YM-3 Cont…		
Sample ID	Depth (cm)	Grain Size (µm)
YM-3-1 31cm	53	504.73
YM-3-1 30cm	54	273.99
YM-3-1 29cm	55	245.17
YM-3-1 28cm	56	384.53
YM-3-1 27cm	57	376.41
YM-3-1 26cm	58	163.98
YM-3-1 25cm	59	587.94
YM-3-1 24cm	60	242.40
YM-3-1 23cm	61	681.76
YM-3-1 22cm	62	376.37
YM-3-1 21cm	63	14.54
YM-3-1 20cm	64	126.22
YM-3-1 19cm	65	181.03
YM-3-1 18cm	66	211.08
YM-3-1 17cm	67	14.10
YM-3-1 16cm	68	152.48
YM-3-1 15cm	69	538.88
YM-3-1 14cm	70	289.47
YM-3-1 13cm	71	440.89
YM-3-1 12cm	72	204.51
YM-3-1 11cm	73	448.19
YM-3-1 10cm	74	107.95
YM-3-1 9cm	75	524.41
YM-3-1 7cm	77	547.94
YM-3-1 5cm	79	408.66
YM-3-1 3cm	81	340.72
YM-3-1 2cm	82	45.03
YM-3-1 1cm	83	39.63

9.4 Mean Grain Size Data, JD Hayes Mill

JD Hayes' Mill Core JDH-1		
Sample ID	Depth (cm)	Grain Size (µm)
JDH-1-1 20cm	1	197.98
JDH-1-1 19cm	2	191.14
JDH-1-1 18cm	3	214.88
JDH-1-1 17cm	4	298.71
JDH-1-1 16cm	5	81.89
JDH-1-1 15cm	6	348.00
JDH-1-1 14cm	7	340.46
JDH-1-1 13cm	8	109.94
JDH-1-1 12cm	9	250.11
JDH-1-1 11cm	10	120.39
JDH-1-1 10cm	11	557.58
JDH-1-1 9cm	12	519.24
JDH-1-1 8cm	13	577.52
JDH-1-1 7cm	14	155.97
JDH-1-1 6cm	15	376.86
JDH-1-1 5cm	16	529.82
JDH-1-1 4cm	17	497.33
JDH-1-1 3cm	18	652.98
JDH-1-1 2cm	19	351.09
JDH-1-1 1cm	20	167.05
JDH-1-1 CC	22	609.29

Core JDH-2		
Sample ID	Depth (cm)	Grain Size (µm)
JDH-2-1 33cm	1	101.02
JDH-2-1 31cm	3	57.12
JDH-2-1 30cm	4	65.66
JDH-2-1 29cm	5	236.08
JDH-2-1 28cm	6	58.23
JDH-2-1 27cm	7	97.25
JDH-2-1 26cm	8	122.88
JDH-2-1 25cm	9	114.14
JDH-2-1 24cm	10	26.19
JDH-2-1 23cm	11	26.09

Core JDH-2 Cont…		
Sample ID	Depth (cm)	Grain Size (µm)
JDH-2-1 21cm	13	22.03
JDH-2-1 19cm	15	22.26
JDH-2-1 17cm	17	25.77
JDH-2-1 16cm	18	30.55
JDH-2-1 15cm	19	56.76
JDH-2-1 14cm	20	27.72
JDH-2-1 13cm	21	24.32
JDH-2-1 11cm	23	24.08
JDH-2-1 9cm	25	21.81
JDH-2-1 7cm	27	24.36
JDH-2-1 5cm	29	17.49
JDH-2-1 3cm	31	21.76
JDH-2-1 1cm	33	21.24
JDH-2-2 73cm	35	24.42
JDH-2-2 71cm	37	17.68
JDH-2-2 70cm	38	205.59
JDH-2-2 69cm	39	201.04
JDH-2-2 68cm	40	92.85
JDH-2-2 67cm	41	237.04
JDH-2-2 66cm	42	215.59
JDH-2-2 65cm	43	229.41
JDH-2-2 64cm	44	187.90
JDH-2-2 63cm	45	261.00
JDH-2-2 61cm	47	JDH-2-2 62cm
JDH-2-2 61cm	47	224.93
JDH-2-2 60cm	48	235.84
JDH-2-2 59cm	49	241.42
JDH-2-2 58cm	50	191.32
JDH-2-2 57cm	51	246.63
JDH-2-2 56cm	52	240.02
JDH-2-2 55cm	53	281.99
JDH-2-2 54cm	54	179.74
JDH-2-2 53cm	55	70.08
JDH-2-2 52cm	56	258.40
JDH-2-2 51cm	57	219.43

Core JDH-2 Cont…		
Sample ID	Depth (cm)	Grain Size (µm)
JDH-2-2 50cm	58	241.75
JDH-2-2 49cm	59	201.75
JDH-2-2 48cm	60	173.41
JDH-2-2 47cm	61	149.14
JDH-2-2 46cm	62	233.48
JDH-2-2 45cm	63	223.58
JDH-2-2 44cm	64	177.93
JDH-2-2 43cm	65	243.42
JDH-2-2 42cm	66	166.48
JDH-2-2 41cm	67	215.42
JDH-2-2 40cm	68	233.39
JDH-2-2 39cm	69	208.33
JDH-2-2 38cm	70	149.94
JDH-2-2 37cm	71	184.37
JDH-2-2 36cm	72	183.86
JDH-2-2 35cm	73	189.43
JDH-2-2 34cm	74	181.37
JDH-2-2 33cm	75	199.78
JDH-2-2 32cm	76	146.96
JDH-2-2 31cm	77	184
JDH-2-2 30cm	78	187.63
JDH-2-2 29cm	79	217.95
JDH-2-2 28cm	80	123.83
JDH-2-2 27cm	81	203.55
JDH-2-2 26cm	82	187.20
JDH-2-2 25cm	83	217.17
JDH-2-2 24cm	84	161.08
JDH-2-2 23cm	85	361.86
JDH-2-2 22cm	86	265.92
JDH-2-2 21cm	87	391.75
JDH-2-2 20cm	88	232.33
JDH-2-2 19cm	89	225.45

Core JDH-2 Cont…		
Sample ID	Depth (cm)	Grain Size (µm)
JDH-2-2 18cm	90	300.84
JDH-2-2 17cm	91	388.26
JDH-2-2 16cm	92	386.13
JDH-2-2 15cm	93	444.03
JDH-2-2 14cm	94	419.54
JDH-2-2 13cm	95	366.34
JDH-2-2 12cm	96	344.79
JDH-2-2 11cm	97	458.41
JDH-2-2 10cm	98	405.10
JDH-2-2 9cm	99	327.67
JDH-2-2 8cm	100	145.44
JDH-2-2 7cm	101	363.18
JDH-2-2 6cm	102	346.90
JDH-2-2 5cm	103	404.67
JDH-2-2 4cm	104	440.17
JDH-2-2 3cm	105	409.89
JDH-2-2 2cm	106	350.09
JDH-2-2 1cm	107	404.07

9.5 Mean Grain Size Data, Mitchell Mill

Mitchell Mill Core MMP-1		
Sample ID	Depth (cm)	Grain Size (µm)
MMP-1-1 32cm	1	24.55
MMP-1-1 31cm	2	30.10
MMP-1-1 30cm	3	25.5
MMP-1-1 29cm	4	650.21
MMP-1-1 28cm	5	17.59
MMP-1-1 27cm	6	877.52
MMP-1-1 26cm	7	29.35
MMP-1-1 25cm	8	657.50
MMP-1-1 24cm	9	22.74
MMP-1-1 23cm	10	46.21
MMP-1-1 21cm	12	21.76
MMP-1-1 20cm	13	503.10
MMP-1-1 19cm	14	305.60
MMP-1-1 18cm	15	25.92
MMP-1-1 17cm	16	17.32
MMP-1-1 16cm	17	240.44
MMP-1-1 15cm	18	1039.36
MMP-1-1 14cm	19	777.55
MMP-1-1 13cm	20	385.72
MMP-1-1 12cm	21	44.74
MMP-1-1 11cm	22	128.67
MMp-1-1 10cm	23	71.09
MMP-1-1 9cm	24	61.83
MMP-1-1 7cm	26	17.98
MMP-1-1 5cm	28	24.52
MMP-1-1 4cm	29	84.60
MMP-1-1 3cm	30	677.97
MMP-1-1 2cm	31	43.17
MMP-1-1 1cm	32	328.38
MMP-1-1 CC	33	237.81

Core MMP-2		
Sample ID	Depth (cm)	Grain Size (µm)
MMP-2-1 52cm	1	91.67
MMP-2-1 51cm	2	42.61
MMP-2-1 50cm	3	107.67
MMP-2-1 49cm	4	269.74
MMP-2-1 48cm	5	107.21
MMP-2-1 47cm	6	44.79
MMP-2-1 46cm	7	373.42
MMP-2-1 45cm	8	69.32
MMP-2-1 44cm	9	22.06
MMP-2-1 43cm	10	30.40
MMP-2-1 42cm	11	50.72
MMP-2-1 41cm	12	42.16
MMP-2-1 40cm	13	38.78
MMP-2-1 39cm	14	27.88
MMP-2-1 37cm	16	25.53
MMP-2-1 35cm	18	25.70
MMP-2-1 33cm	20	22.22
MMP-2-1 31cm	22	21.67
MMP-2-1 29cm	24	16.42
MMP-2-1 27cm	26	18.41
MMP-2-1 25cm	28	17.12
MMP-2-1 24cm	29	25.29
MMP-2-1 23cm	30	34.88
MMP-2-1 22cm	31	173.22
MMP-2-1 21cm	32	40.36
MMP-2-1 19cm	34	22.02
MMP-2-1 18cm	35	615.08
MMP-2-1 17cm	36	639.88
MMP-2-1 16cm	37	476.88
MMP-2-1 15cm	38	190.17
MMP-2-1 14cm	39	37.80
MMP-2-1 13cm	40	27.40
MMP-2-1 11cm	42	13.71
MMP-2-1 10cm	43	151.18

Core MMP-2 Cont…		
Sample ID	Depth (cm)	Grain Size (µm)
MMP-2-1 9cm	44	410.04
MMP-2-1 8cm	45	331.62
MMP-2-1 7cm	46	51.75
MMP-2-1 6cm	47	15.49
MMP-2-1 5cm	48	11.52
MMP-2-1 3cm	50	19.49
MMP-2-1 1cm	52	19.10
MMP-2-1 CC	54	201.46
MMP-2-2 55cm	55	272.28
MMP-2-2 54cm	56	495.14
MMP-2-2 53cm	57	13.02
MMP-2-2 52cm	58	539.92
MMP-2-2 51cm	59	482.02
MMP-2-2 50cm	60	301.70
MMP-2-2 49cm	61	209.81
MMP-2-2 48cm	62	512.44
MMP-2-2 47cm	63	562.06
MMP-2-2 46cm	64	560.59
MMP-2-2 45cm	65	342.73
MMP-2-2 44cm	66	82.23
MMP-2-2 43cm	67	22.72
MMP-2-2 41cm	69	17.47
MMP-2-2 39cm	71	16.02
MMP-2-2 37cm	73	15.81
MMP-2-2 36cm	74	26.98
MMP-2-2 35cm	75	72.26
MMP-2-2 34cm	76	141.63
MMP-2-2 33cm	77	15.42

9.6 Point Count Data

Sample ID	Seeds	% Seeds	Wood	% Wood	Acquatic Material	% Acquatic Material	Charcoal	% Charcoal	Fly Ash	% Fly Ash	Total
Background Sediments											
YM-1-1 17cm	5	2.49	21	10.45	21	10.45	126	62.69	28	13.93	201
MMP-1-1 31cm	3	1.83	16	9.76	13	7.93	119	72.56	13	7.93	164
BM-2	0	0.00	58	30.37	0	0.00	131	68.59	2	1.05	191
MMP-2-1 39cm	10	5.62	47	26.40	11	6.18	108	60.67	2	1.12	178
RC-11	2	1.27	31	19.75	3	1.91	112	71.34	9	5.73	157
YM-3-1 57cm	7	3.91	24	13.41	10	5.59	110	61.45	28	15.64	179
RC-18	8	5.63	15	10.56	2	1.41	104	73.24	13	9.15	142
JDH-1-1 13cm	6	5.61	64	59.81	1	0.93	34	31.78	2	1.87	107
RC-2	1	0.66	22	14.47	6	3.95	99	65.13	24	15.79	152
JDH-2-1 21cm	6	3.53	10	5.88	2	1.18	123	72.35	29	17.06	170
RC-4	4	2.70	16	10.81	2	1.35	102	68.92	24	16.22	148
MEAN	4.73	3.02	29.45	19.24	6.45	3.72	106.18	64.43	15.82	9.59	162.64
Event Layers											
BM-1	0	0.00	88	88.00	2	2.00	10	10.00	0	0.00	100
RC-3	0	0.00	6	12.24	1	2.04	41	83.67	1	2.04	49
YM-1-1 14cm	41	21.35	62	32.29	6	3.13	76	39.58	7	3.65	192
JDH-2-1 29cm	8	8.51	26	27.66	3	3.19	53	56.38	4	4.26	94
BM-4	1	0.58	92	53.80	1	0.58	67	39.18	10	5.85	171
JDH-1-1 15cm	0	0.00	25	49.02	1	1.96	21	41.18	4	7.84	51
MMP-2-1 49cm	1	1.00	95	95.00	0	0.00	3	3.00	1	1.00	100
RC-10	0	0.00	12	27.27	0	0.00	30	68.18	2	4.55	44
RC-6	1	0.66	50	33.11	1	0.66	85	56.29	14	9.27	151
YM-3-1 47cm	0	0.00	80	80.00	1	1.00	18	18.00	1	1.00	100
MMP-1-1 27cm	12	4.49	89	33.33	1	0.37	150	56.18	15	5.62	267
MEAN	5.82	3.33	56.82	48.34	1.55	1.36	50.36	42.88	5.36	4.10	119.91

9.7 FTIR Peak Locations

	Background Sediments									
	Sample ID:									
Mineral Present	RC-2	RC-4	RC-7	BM-2	YM-1-1 11cm	YM-3-1 57cm	MMP-1-1 31cm	MMP-2-1 39cm	JDH-1-1 13cm	JDH-2-1 21cm
Montmorillonite	1034, 3621	1032, 3620	1032, 3621	1033, 3422, 3621	1032, 3620	1033, 3620	915, 1032, 1090, 3620	1033, 3621	1036, 1090, 3621	1032, 3620
Kaolinite	431, 470, 913, 1007, 3621	470, 912, 1008, 1032, 3620	432, 471, 912, 1007, 1032, 3621	432, 470, 913, 1007, 1032, 3621	431, 471, 913, 1007, 1032, 3620	471, 913, 1008, 1032, 3620, 3695	470, 1008, 1032, 3620	432, 470, 913, 1008, 1100, 3621, 3695	431, 470, 912, 1008, 3621, 3695	432, 470, 912, 1008, 1032, 1100, 3620
Kaolinite, Illite					753				753	
Kaolinite, Illite, Montmorillonite		693	692	693	694			695	692	693
Kaolinite, Halloysite			795				795	795		795
Quartz		780	778		779	798	778	512, 778		778
Biotite				3590					646	
Biotite, Montmorillonite									1115	
Biotite, Montmorillonite, Muscovite					1165	1168				
Chlorite				3560	3570					
Chlorite, Illite						987				
Chlorite, Illite, Quartz										
Calcite, Dolomite										
Albite	700,773, 794	701, 780, 794		700, 776, 793						
Halloysite			692	941					692, 941	

	Sand Layers										
	Sample ID:										
Mineral Present	RC-3	RC-5	RC-10	BM-1	YM-1-1 14cm	YM-3-1 47cm	MMP-1-1 27cm	MMP-2-1 49cm	YM-1-1 13cm	JDH-2-1 15cm	JDH-2-1 29cm
Montmorillonite	1033, 3620	1032, 3620	1036, 3426, 3620	1033	1033, 3620	1033, 3621			1033, 1100, 3620	1033, 3620	
Kaolinite	432, 471, 913, 1007, 3620	432, 470, 913, 1007, 1032, 3620	431, 470, 913, 1008, 3620		432, 470, 913, 1007, 1100, 3620	431,470, 913, 1007, 3622	432, 471, 913, 1008, 1032, 3620	432, 470, 913, 938, 1008, 1032, 3621	432, 470, 913, 1007, 1100, 3620,	432, 470, 913, 1007, 1100, 3620	432, 470, 912, 1007, 1032, 1100, 3619
Kaolinite, Illite	753		753								
Kaolinite, Illite, Montmorillonite	693	693	693	693	693	693	694	694	693	692	692
Kaolinite, Halloysite		795	795			795			795	795	
Quartz	778	512, 778	512, 779	778	778, 799	778	778	778	778	778	512, 778
Biotite	646							646			
Biotite, Montmorillonite							1115	1115			
Biotite, Montmorillonite, Muscovite				1170							
Chlorite	3485					3569					
Chlorite, Illite											
Chlorite, Illite, Quartz				1083							
Calcite, Dolomite				1425							
Albite	753, 778, 796	700, 795			700,778, 799		700, 778, 796		700, 776, 794	700, 776, 795	700, 778, 794
Halloysite	692	941	692, 941			692, 941	941, 1094	1094	692, 941		